1-1-2012

Development of an Atmospheric Pressure Laser Induced Fluorimeter (AP-LIF) for NO_2 and Application of AP-LIF for Study of Heterogeneous NO_2 Chemistry

Jeremy Parra
Portland State University

Development of an Atmospheric Pressure Laser Induced Fluorimeter (AP-LIF) for NO_2 and Application of AP-LIF for study of Heterogeneous NO_2 Chemistry

by

Jeremy Parra

A dissertation submitted in partial fulfillment of the
requirements for the degree of

Doctor of Philosophy
in
Applied Physics

Dissertation Committee:
Linda A. George, Chair
Dean B. Atkinson
Aslam Khalil
Andres La Rosa
Andrew Rice
Jiunn-Der Duh

Portland State University

Abstract

Nitrogen dioxide (NO_2) is a pollutant of interest for study both because of its controlling role in the oxidant capacity of the atmosphere and the health risks it poses. Concerns about the health effects of NO_2 and its role in forming deleterious atmospheric species have made it desirable to have low-cost, sensitive ambient measurements of NO_2. A continuous-wave laser-diode laser-induced fluorescence (LIF) system for NO_2 was developed here which operates at ambient pressure, thereby eliminating the need for an expensive pumping system. The current prototype system has achieved sensitivity several orders of magnitude beyond previous efforts at ambient pressure (limit of detection of 2 ppb, 60 s averaging time). Ambient measurements of NO_2 were made in Portland, Oregon using both the standard NO_2 chemiluminescence method and the LIF instrument and showed good agreement (r^2 = 0.92).

In addition, investigations into surface mediated chemistry involving oxides of nitrogen (namely, NO_y) have stimulated new inquiry into potential heterogeneous sources of NO_2 as well as challenged the stability of permanent sinks for NO_2. The possibility that surface mediated chemistry plays a significant role in NO_y chemistry in urban air has for the past few decades received considerable attention. The AP-LIF NO_2 instrument is uniquely suited to measure surface chemistry under near ambient conditions.

The so called 'renoxification' reaction of gaseous NO with surface bound HNO_3 yielding NO_2 ($2\,HNO_3(\text{surface}) + NO \longrightarrow 3\,NO_2 + H_2O(\text{surface})$) was

suggested as a potentially important source of NO_2 which also degraded the stability of nitric acid as a sink of active oxides of nitrogen. Yet, there is disagreement in the literature as to the importance of this reaction. The disagreement stems from differing measurements of the rate for the renoxification reaction. Because there are differences in experimental setups no one research group has studied the renoxification reaction under ambient conditions, i.e., at moderate concentrations of NO_y and in a static cell held at 1 atm. In this work, the production of NO_2 was measured using a novel AP-LIF. This setup made it possible to measure the rate of production of NO_2 due to the heterogeneous reaction of NO with HNO_3 under ambient conditions. Under these conditions it was found that renoxification due to gas-phase NO on surface HNO_3 is not a significant source of NO_2. However, this study did show the importance of water vapor in the renoxification of surface HNO_3.

To Amy, my helpmate and best friend.
Growing up with you has provided me
the metric by which to grow up well.

It is the glory of GOD to conceal a matter;
to search out a matter is the glory of kings.

Acknowledgments

I owe my deepest gratitude to my advisor and teacher, Dr. Linda A. George, for allowing me the opportunity to work toward this goal. She patiently stood by as I broke many things in her lab. By her encouragement and balanced approach to mentoring I was able to grow from tinkerer to experimentalist. I hope that in the end I created more than I destroyed.

My great appreciation also goes to Dr. Andres La Rosa who gave me an early break in his lab and graciously encouraged me to pursue a good environment in which to complete my graduate studies. I would also like to extend my gratitude to Drs. Dean B. Atkinson and Tom Hard for their time and advice on numerous topics.

A great deal of thanks goes to my peers, whom I have had the privilege to journey with in this endeavor. Especially, I would like to thank Tom Dornan, Greg Bostrom, Derek Nowak and Jimmy Radney for sharing ideas, criticisms, and cold beverages.

I owe more to my parents, Jorge and Maria Parra, than I could ever pen down, but in this I owe a great debt, that while many times I was found wandering they never doubted that I was lost.

Table of Contents

List of Tables

List of Figures

Chapter 1

INTRODUCTION

Nitrogen oxides have a ubiquitous role in the chemistry of the clean and polluted atmosphere. Although many direct and indirect measurement techniques exist, low-pressure laser-induced fluorescence (LIF) has the advantage of being both a direct and sensitive measure of NO_2. Laser diodes have dramatically reduced the cost and energy requirements of NO_2 LIF, yet the low-pressure regime of these systems adds significant cost, energy use, and bulk via their pumping systems. This investigation examines the use of an Atmospheric Pressure Laser Induced Fluorimeter (AP-LIF), developed here, as a sensitive and direct method of measuring low levels of NO_2 in the troposphere as well as its application to in situ chemical kinetics studies involving NO_2 at atmospheric pressures and concentrations.

1.1 Importance of Atmospheric Oxides of Nitrogen

The focus of much of tropospheric air chemistry is on oxides of nitrogen and volatile organic compounds (VOCs) as well as the secondary pollutants which

are formed through photochemical reactions (Atkinson, 2000). The principal forms of chemically active nitrogen oxides in the troposphere are nitric oxide (NO) and nitrogen dioxide (NO_2). The sum concentration in the atmosphere of these two compounds is called NO_x. In the troposphere NO_x compounds are important in controlling the concentration of the two primary day-time oxidants, hydroxyl radical (OH) and ozone (O_3), as well as the night-time oxidant, nitrate radical (NO_3)(Figure 1.1).

Nitrogen oxides are released into the atmosphere through natural and anthropogenic means. The largest source of nitrogen oxides is the release of nitrous oxide (N_2O) via microbial processes in soil and water. In the troposphere N_2O is not chemically reactive but it is an important agent in controlling stratospheric ozone. N_2O absorbs wavelength shorter than 290 nm found in the stratosphere and dissociates to form N_2 and electronically excited $O(^1D)$:

$$N_2O + h\nu \longrightarrow N_2 + O(^1D) \qquad (R\,1.1)$$

.

This reaction is followed by reaction R 1.2 which is primarily responsible for the production of reactive oxides of nitrogen in the stratosphere.

$$O(^1D) + N_2O \longrightarrow 2\,NO \qquad (R\,1.2)$$

The most significant nitrogen oxide species emitted anthropogenically is nitric oxide (NO), which is produced when N_2 and O_2 react during high-

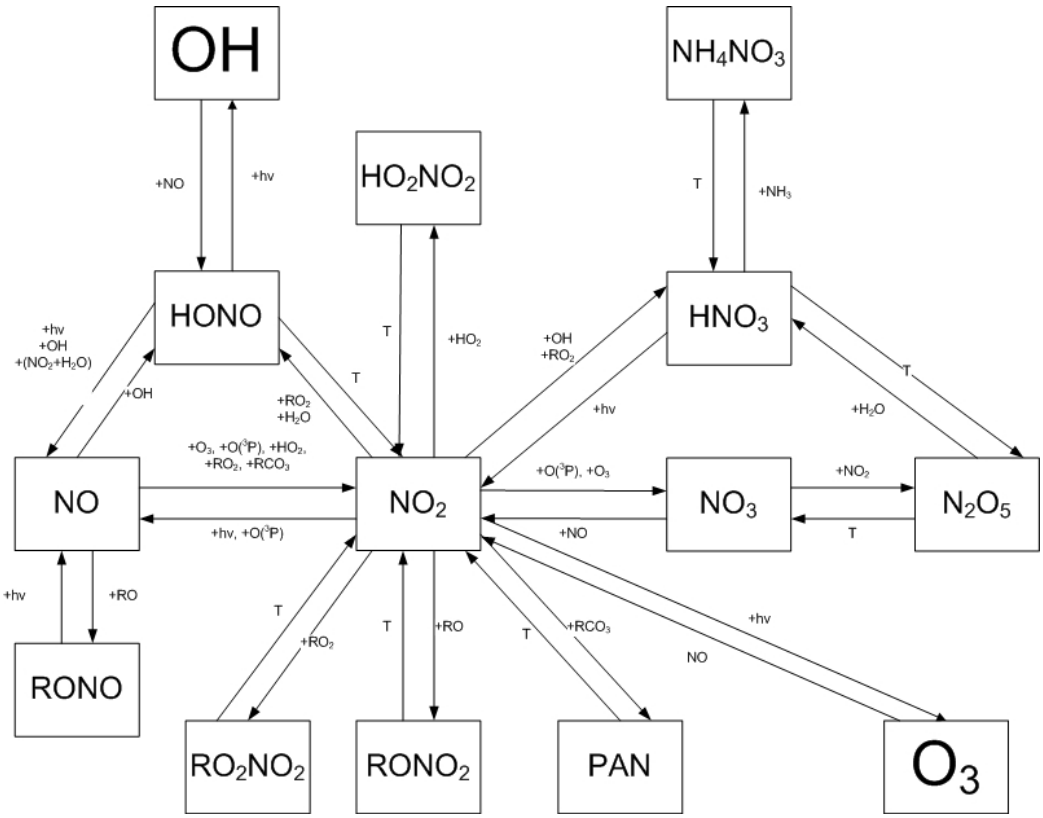

Figure 1.1: Nitrogen oxide reaction scheme.

temperature combustion processes. Smaller amounts of NO_2 are also produced when NO is further oxidized. On a global scale, anthropogenic emissions make up 63% (33 TgN/yr) of the total inventoried sources for NO_x, biomass burning making up another 14 % (7.1 TgN/yr), with the remaning sources of NO_x due to microbial activity in soils and production from lightening discharges (IPCC, 2001).

Photochemical oxidation of natural and anthropogenic emissions is the means by which the atmosphere maintains a near constant atmospheric composition. Understanding changes to this balance requires a better understanding of homogeneous and heterogeneous chemistry of the atmosphere as well as sound measurements with high spatial and temporal accuracy.

The hydroxyl radical is the chief agent in preventing the buildup of hydrocarbons (RH) and other pollutants in the troposphere. Hydrocarbon removal is initiated by oxidation with OH:

$$\mathrm{RH} + \mathrm{OH} \longrightarrow \mathrm{R} + \mathrm{H_2O}. \qquad (\mathrm{R}\,1.3)$$

The oxidized hydrocarbon, in the presence of sunlight and further reaction with OH, is either removed from the atmosphere as a soluble organic compound by wet or dry deposition or completely oxidized to CO_2. One source of the hydroxyl radical in the polluted atmosphere is the photolysis of nitrous acid (HONO):

$$\mathrm{HONO} + \mathrm{h}\nu \longrightarrow \mathrm{OH} + \mathrm{NO}(_{300}\mathrm{nm}{<}\lambda{<}405\,\mathrm{nm}). \qquad (\mathrm{R}\,1.4)$$

Reaction R 1.4 happens very fast during the day so that significant concentrations are not developed. Yet, the build up of HONO during the evening and subsequent photolysis in the morning has been reported to be a major source of OH in the polluted environment (Alicke et al., 2002; Aumont et al., 2003; Finlayson-Pitts, 2000; Harrison et al., 1996; Kotamarthi et al., 2001; Lammel and Cape, 1996; Perner and Platt, 1979; Platt and Perner, 1980; Schiller et al., 2001; Stutz et al., 2002; Winer and Biermann, 1994; **?**). Sources of HONO are still not completely understood. Discrepancies between field measurements and models based on known gas chemistry vary up to an order of magnitude (Acker et al., 2005, 2006a,b; He et al., 2006; Kleffmann et al., 2005). In addition to direct emissions, heterogeneous pathways are the most likely source of HONO in the boundary layer (Finlayson-Pitts, 2000). Because of its role in forming OH, understanding the sources and sinks of HONO is critical for understanding the polluted atmosphere.

Another critical atmospheric oxidant is ozone which initiates the oxidation of some hydrocarbons (particularly alkenes) and also oxidizes NO_2 to form the NO_3 radical (see Figure 1.1). In the clean troposphere, photolysis of ozone in the presence of water vapor is a major source of OH radicals, reaction R 1.5 followed by reaction R 1.6.

$$O_3 + h\nu(\lambda{<}310\,\mathrm{nm}) \longrightarrow O(^1D) \qquad \text{(R 1.5)}$$

$$O(^1D) + H_2O \longrightarrow 2\,HO \qquad \text{(R 1.6)}$$

Elevated levels of ozone can be detrimental to human and vegetative health because ozone destroys human and plant cell tissue (Bennett et al., 1975; Reich et al., 1990).

In the troposphere, ozone is formed via the photolysis of NO_2 in oxygen. Reaction R 1.7 followed by reaction R 1.8.

$$NO_2 + h\nu \longrightarrow NO + O \tag{R 1.7}$$

$$O + O_2 \xrightarrow{M} O_3 + M \tag{R 1.8}$$

O_3 can then react with NO to regenerate NO_2 and O_2 (reaction R 1.9):

$$NO + O_3 \longrightarrow NO_2 + O_2. \tag{R 1.9}$$

This null cycle is known as the Photostationary State (PSS); significant side reactions can cause an imbalance in the PSS resulting in a net production (reactions R 1.10 and R 1.11) or loss of ozone, e.g., ozone + alkene $\longrightarrow$ products.

$$RO_2 + NO \longrightarrow RO + NO_2 \tag{R 1.10}$$

$$HO_2 + NO \longrightarrow HO + NO_2 \tag{R 1.11}$$

NO_2 can also be further oxidized by O_3 to form the nitrate radical:

$$O_3 + NO_2 \longrightarrow NO_3 \qquad \text{(R 1.12)}$$

.

NO_3 strongly absorbs throughout the visible region and is quickly photolyzed during the day (reactions R 1.13 and R 1.14); with a lifetime of just 5 seconds for overhead sun (Orlando et al., 1993). In the nighttime however NO_3 can build up to significant mixing ratios.

NO_3 reacts quickly with unsaturated hydrocarbons to form peroxy radicals (RO_2 and HO_2). RO_2 reacts with NO to form NO_2 and jump start the morning ozone formation in polluted environments (Salisbury et al., 2001). NO_3 radical reaction with some hydrocarbons has also been found to be an efficient pathway for the formation of condensible compounds leading to formation of secondary organic aerosols (Hoffmann et al., 1997).

$$NO_3 + h\nu \longrightarrow NO_2 + O \qquad \text{(R 1.13)}$$

$$NO_3 + h\nu \longrightarrow NO + O_2 \qquad \text{(R 1.14)}$$

Although most of the anthropogenic sources of NO_x are found within the urban setting, formation and long range transport of organic nitrates (e.g. R 1.15 and R 1.16) are responsible for considerable increase of reactive nitrogen oxides in otherwise unpolluted regions (Singh et al., 1998).

$$RO_2 + NO \longrightarrow RONO_2 \qquad \text{(R 1.15)}$$

$$RO_2 + NO_2 \longrightarrow ROONO_2 \qquad \text{(R 1.16)}$$

Peroxyacetyl nitrate, $CH_3C(O)OONO_2$, also known as PAN is the most abundant organic nitrate in the troposphere and contributes significantly to the total tropospheric abundance of reactive oxides of nitrogen. Because it is quite stable at low temperatures PAN is an important means of transporting NO_x over large distances. At higher temperatures and through photolysis PAN can reproduce NO_x species far from the original source. By convention NO_y represents the sum of all reactive nitrogen-containing species, e.g., (NO_y = NO_x + HNO_3 + PAN + HONO + NO_3 + N_2O_5 + organic nitrates +...). After being transported up to hundreds of kilometers NO_y species can be converted back to NO_x by the following reactions (Hov and Larssen, 1984; Moxim, 1990).

$$N_2O_5 + h\nu \longrightarrow NO_2 + NO_3 \qquad \text{(R 1.17)}$$

$$RO_2NO_2 + M \longrightarrow RO_2 + NO_2 + M \qquad \text{(R 1.18)}$$

$$NO_3 + h\nu \longrightarrow NO_2 + O \qquad \text{(R 1.19)}$$

$$NO_3 + h\nu \longrightarrow NO + O_2 \qquad \text{(R 1.20)}$$

If these species are transported from polluted areas and subsequently converted to NO_x they can lead to formation of tropospheric ozone in remote regions.

Many reactions of nitrogen oxides that are slow in the gas phase occur

at significant rates on surfaces. Current understanding of magnitude and mechanisms of heterogeneous reactions in the troposphere are limited, due in part to the wide range of surfaces available for this chemistry. As an example, while the sources of HONO are still not completely understood, in addition to direct emissions, heterogeneous pathways are the most likely source of HONO in the boundary layer (Finlayson-Pitts, 2000). Because of its importance as a daytime source of HO (Winer and Biermann, 1994; Alicke et al., 2002; Aumont et al., 2003; Harrison et al., 1996; Perner and Platt, 1979; Platt and Perner, 1980; Lammel and Cape, 1996; Finlayson-Pitts, 2000; Schiller et al., 2001; Kotamarthi et al., 2001; Alicke et al., 2002; Stutz et al., 2002), much research has been focused on finding plausible heterogeneous sources for HONO (Fairbrother et al., 1997; George et al., 2005; Handley et al., 2007; Ramazan et al., 2006; Saliba et al., 2000). The heterogeneous hydrolysis of NO_2 which forms HONO has been cited in laboratory studies as a significant source of HONO (Alicke et al., 2003):

$$2\,NO_2 + H_2O \longrightarrow HONO + HNO_3(ads)\,\cdot \qquad (R\,1.21)$$

Hydrolysis of NO_2 (reaction R 1.21) alone is not sufficient in explaining the observed night-time build up of HONO in polluted air-masses (Moussiopoulos et al., 2000). Thus other heterogeneous pathways are expected to be found.

Nitrogen oxides are readily converted to nitric acid via the reaction with HO:

$$HO + NO_2 + M \longrightarrow HNO_3 + M \qquad (R\,1.22)$$

HNO_3 is removed form the atmosphere through wet and dry surface deposition of (Logan, 1983). In this process HO is removed from the atmosphere which reduces the consumption of hydrocarbons. If the nitric acid remains on the surface then this reaction contributes to the permanent removal of oxides of nitrogen from the atmosphere and is a significant step in terminating the ozone formation cycle. However, recent evidence has pointed to the possibility of HNO_3 being reduced back to photochemically active nitrogen (e.g. NO, NO_2, HONO) via surface chemistry in the so called 'renoxification' process (Ramazan et al., 2006). One such possible reaction is the production of HONO (R 1.23) and gaseous NO_2 when NO interacts with HNO_3 on surfaces suggesting that surface bound HNO_3 is not a permanent sink for nitrogen oxides.

$$HNO_3(ads) + NO \longrightarrow HONO(ads) + NO_2 \qquad (R\,1.23)$$

There is general disagreement in the literature about the importance of reaction R 1.23 (Kleffmann et al., 2004; Rivera-Figueroa et al., 2003; Saliba et al., 2001). Even so other heterogeneous pathways may exist which form HONO and other reactive forms of nitrogen oxides (Ammann et al., 1998; George et al., 2005; Gutzwiller et al., 2002). Work by Diamond and coworkers (Diamond et al., 2000; Gingrich and Diamond, 2001; Hodge et al.,

2003; Liu et al., 2003) has shown that organic layers exists on the surface of most impervious materials, which may react with gas-phase oxidants. It is critical to determine the importance of heterogeneous chemistry of nitrogen oxides, especially in the boundary layer where many surfaces exist, e.g., suspended particles, soils, plants, snow and building materials.

Nitrogen oxides also play a role in aerosol formation and composition. As an example, sea salt particles containing sodium chloride (NaCl) can interact with oxides of nitrogen such as nitric acid:

$$\mathrm{NaCl(s) + HNO_3(g) \longrightarrow HCl(g) + NaNO_3(s)} \cdot \qquad \text{(R 1.24)}$$

In this reaction chloride is replaced with nitrate. This initial reaction does not have a significant affect on the particle morphology(Finlayson-Pitts, 2000), but if exposed to water vapor and subsequently dried the surface nitrate can reorganize and may be responsible for small particles in the marine boundary layer (Mouri et al., 1995). NO_y also has a role in the formation of secondary aerosol formation(SOA). Especially in urban settings where gas-phase organics are exposed to large amounts of oxidants even relatively simple organics from biogenic emissions have amble opportunity to form multifunctional organics. Some of these have sufficiently low vapor pressures that they will exist in the particle phase. As an abundant source of oxidation in these settings NO_y has a significant role in SOA formation. Although this work does not focus on such reactions, gas-phase/ particle partitioning and the

formation of organic aerosols through NO_y oxidation is something that the AP-LIF instrumentation can be suited for (see chapter 5).

1.2 Health effects of NO_x

Nitrogen dioxide is a pollutant of interest for study both because of its controlling role in the oxidant capacity of the atmosphere and the health risks it poses, especially for vulnerable populations. NO_2 acts as a strong oxidant and may lead to toxicity in the lungs leading to injury and death. Extremely high-dose exposure (as in building fires) can result in pulmonary edema and diffuse lung injury. One time-series analysis demonstrated an association between NO_2 concentrations in metropolitan Los Angeles and cardiovascular and pulmonary hospital admissions (Linn et al., 2000). The most significant associations between NO_2 in outdoor air pollution and asthma and lower respiratory disease tend to occur in children (Gillespie-Bennett et al., 2011). Studies have demonstrated that mild asthmatics' early and late allergic responses to mite allergens were exacerbated following exposure to relatively high concentrations of NO_2 (0.2–0.5 ppm), and that NO_2 triggered an inflammatory reaction by human nasal mucosal cells in an organ culture (Bascom et al., 1996; Tunnicliffe et al., 1994). Some studies found stronger associations between exposure and symptoms (e.g., chest tightness and dyspnea on exertion) during the cumulative lags following exposure than immediately upon exposure (Anderson et al., 1998; Schierhorn et al., 1999). It is not only high concentrations of NO_2 which cause significant health effects. Re-

search indicates that levels of NO_2 typically found in urban environments (20-100 ppb) may cause increased bronchial reactivity in some asthmatics, decreased lung function in patients with chronic obstructive pulmonary disease and increased risk of respiratory infections, especially in young children (Gillespie-Bennett et al., 2011).

In developed countries up to 90% of people's time may be spent indoors (Tunnicliffe et al., 1994). This coupled with the fact that indoor concentrations of NO_2, resulting from the use of gas for cooking or space and water heating, are often higher than outdoor concentrations (Dennekamp et al., 2001) exacerbates the issue for many vunerable populations. NO_2 concentrations were 4 to 7 times higher in homes with gas stove, with an average NO_2 concentration below the national standard of 100 μg m^{-3}, but short-term peaks exceeded 1100 μg m^{-3} (Weinberger et al., 2001).

1.3 Measurement Techniques for NO_2 and NO_y

While no counties in the US are currently in non-attainment for NO_2, the US EPA has recently announced sweeping new regulations aimed at reducing NO_x levels by 2015 (Environmental Protection Agency, 2005). Therefore, accurately measuring the concentration of NO_2, as mandated under the 1990 Clean Air Act Amendments, Section 182 (c)(1) (Demerjian, 2000), will become increasingly important. In addition to the regulatory purposes of monitoring, ambient measurements are also used by air quality models(AQM) for characterization and prediction of future high ozone episodes. Tropospheric

measurements of NO_2 are now commonplace and typically accomplished using techniques based on NO determination. NO_x chemiluminescence (CL-NO_x), for example, measures NO_2 by first reducing NO_2 to NO through a catalytic or photolytic process (Kelly et al., 1980; Ridley et al., 1988). Nitric oxide is then measured by reaction with excess ozone or luminol and measuring the chemiluminescence emitted by excited NO_2 formed. The technique is simple and relatively reliable. The detection sensitivity benefits from small background signal levels because no light source is necessary to initiate the fluorescence.

Commercial chemiluminescence devices exist which have high sensitivity (sub-ppb averaged over several minutes), but the accuracy of these measurements is limited due to interferences. The most significant issue with standard CL-NO_x monitors is their inability to directly and specifically detect NO_2. It has been well established that other gas phase NO_y compounds are converted by molybdenum oxide catalysts to NO and therefore can be reported as NO_2 by a standard CL-NO_x monitor (Williams et al., 1998; Winer et al., 1974). Positive interferences in the measurement of NO_2 may lead to the false classification of an urban area as being in non-attainment. Photolysis can be used to more specifically convert NO_2 to NO, which avoids using a metal catalyst while still employing the chemiluminescence reaction (Gao et al., 1994). In photolytic chemiluminescence (P-CL) a powerful UV light source (100 W Hg arc lamp or high power LEDs) is used to decompose NO_2 into NO and an oxygen atom. Ozone is then reacted with this NO to form

excited NO_2 which emits light as it is deactivated. In P-CL long residence times in the detection cell can lead to unwanted thermal or surface mediated decomposition of other NO_y species. Conversion efficiency is the primary concern for the P-CL; to achieve maximum sensitivity the residence time and the photon flux can be increased to ensure that NO_2 is photolyzed (Kley and McFarland, 1980). Long residence times in the detection cell can increase unwanted thermal or surface mediated decomposition of NO_y species. For this reason powerful light sources are used; these light source create excessive heat and steps must be taken to keep the system cool (Pollack et al., 2010). An artifact of P-CL instrumentation is the surface deposition of nitrogen oxide such as HNO_3 which will decompose and yield a signal even when a clean air sample is present. A 'clean air' step is required to account for this background (Kley and McFarland, 1980).

NO_2 can also be measured directly using optical absorption techniques. Differential Optical Absorption Spectroscopy (DOAS) is a direct measurement technique but requires long spatial averaging (Platt and Perner, 1980). The requirement of a long path length is obviated by using cavity ring down (CRD) (Osthoff et al., 2006), but a highly stable cavity is required for this technique. The Tunable Infrared Laser Differential Absorption Spectroscopy (TILDAS) technique for measuring NO_2 employs a low volume, long path length astigmatic Herriott multipass absorption cell (Macmanus et al., 1995) with liquid nitrogen cooled laser infrared diodes and detectors (Li et al., 2004). The laser line width is small compared to the width of the absorption

feature and the laser frequency position is rapidly swept over an entire absorption feature of NO_2. Courtillot et al. (2006) have developed an optical feedback cavity-enhanced absorption spectrometer (OF-CEAS) operating in the blue region of the visible spectrum (400 nm) where NO_2 has large absorption cross sections. The technique relies on optical feedback from the cavity to reduce the laser line width to well below the cavity-mode line width. In this arrangement excitation of cavity resonance is optimal. Direct measurements of NO_2 down to the hundreds of ppt are possible with this technique. A newer technique, Cavity Attenuated Phase Shift (CAPS) spectroscopy, has shown the potential to provide accurate spectroscopic measurements of NO_2 (0.3 ppb detection limit in <10 s) at a reasonable cost (Kebabian et al., 2005).

Laser Induced Fluorescence (LIF) is also a direct measurement technique for NO_2. LIF has a relatively simple experimental arrangement and excellent sensitivity at fast averaging intervals(15 pptv at 10 sec) (Thornton et al., 2000). LIF techniques for ambient NO_2 measurements typically employ the Fluorescence Assay with Gas-Expansion (FAGE) technique (Thornton et al., 2000; Cleary et al., 2002; Fong and Brune, 1997; Taketani et al., 2007; George and O'Brien, 1991). In this technique analyte is drawn into a low pressure ($\sim$1 torr) cell using high volume vacuum pumps, the analyte is subsequently radiated with laser light. Because of its relatively long radiative lifetime at low pressures ($\sim$100 μ s at 35 mtorr and 585 nm excitation) the fluorescence signal can be recorded sometime after the laser has been shut-off, allowing for

a high signal to noise ratio. Although laser diodes have dramatically reduced the cost and energy requirements of NO_2 LIF (Taketani et al., 2007), the low-pressure regime of these systems adds significant cost, energy use, and bulk via their pumping systems.

Several techniques have been used to investigate NO_2 surface reactions. Finlayson-Pitts and co-workers in studying NO_2 hydrolysis used a reactor equipped with a multi-pass Fourier transform infrared (FTIR) white-cell spectrometer which was cable of measuring NO, NO_2, and HONO, but had a very high limit of detection (20 ppm) (Finlayson-Pitts et al., 2003; Ramazan et al., 2006). George et al. (2005) used a flow tube reactor to investigate the photochemical increase in NO_2 uptake on solid organic compounds. In this investigation a mass spectrometer was used to measure the gases at high concentrations while a long pass absorption photometer (LOPAP) and chemiluminescence monitor were used at more atmospherically relevant concentrations of NO_x and HONO. Teklemariam and Sparks (2006) used a chemiluminescence analyzer to measure NO_2 leaf fluxes. One common drawback for all of these methods is that the sample must be drawn into a detection chamber. Under some circumstances it is not possible to draw a sample without greatly disturbing the system under study. In recent years there has been much interest in methods of detecting minor species, such as NO_2, in combustion processes. In order to do so, an in situ NO_2 detection method is needed which can detect low concentrations in an environment at or above 1 atm. Mann et al. (1996) compared two techniques with these capabili-

ties, degenerate four wave mixing (DFWM) and LIF. DFWM is a non-linear wave mixing technique which allows for a very high signal-to-noise(SNR) ratio (Mann et al., 1996; Smith et al., 1995), and has the distinct advantage that the SNR goes up with pressure. Although DFWM has a much better SNR than LIF at atmospheric pressure (Mann et al., 1996), LIF presents a much easier setup. Both techniques can utilize charged-coupled devices (CCD) in order to produce images of NO_2 concentration profiles. By operating at atmospheric pressure the AP-LIF system can be used to study many systems in situ for which low pressure is not suited, e.g., flame and combustion chemistry, surface uptake and release from snow-pack and leafs as well as many other surface reactions. Also, by operating at atmospheric pressure the need for a bulky and costly vacuum pump would be obviated; in this case the development of a sensitive and direct NO_2 technique which is compact and low cost would be beneficial for making ambient measurements. A NO_2-LIF system can also be utilized as a 'back-end' detector of an NO_y ambient monitor. With the removal of the expensive high-capacity pump, separate cells for each constituent of NO_y can be employed, thereby eliminating the complexity and potential chemical artifacts associated with switching between NO_y modes (Day et al., 2002).

Chapter 2

DEVELOPMENT OF AP-LIF FOR NO_2

2.1 Laser Induced Fluorescence of NO_2

Laser-induced fluorescence (LIF) is the emission from atoms or molecules which have been excited by laser radiation. Because of this, LIF has the advantage of being both a direct and selective measure of an analyte. When a molecule resonantly absorbs a photon of a given wavelength(λ) from a laser beam, it is put into an excited energy state. In this state the molecule is unstable and will either decay spontaneously, giving off photons ($I_F(\lambda_F)$), or may lose its energy to a quenching molecule in a non-radiative energy transfer. Some of the laser light ($I_L(\lambda)$) will be scattered by bath molecules and will contribute to the background ($I_S(\lambda)$). In a typical setup, the fluorescence signal is measured at 90° to a collimated laser beam (see Figure 2.1), and both fluorescence photons (or signal) and scattered source photons (or noise) will be detected. Much consideration is thus spent in maximizing the signal detected whilst reducing the noise so that a higher signal-to-noise (SNR) ratio may be achieved. As a first step in noise reduction, the fluores-

cence signal is typically collected at 90° degree to the laser beam with the laser polarized parallel to the plane of the detector. According to Rayleigh scattering theory scattered photons arriving at the detector will be minimal under this arrangement, Figure 2.2.

Lasers are excellent excitation sources for doing spectroscopy on molecules. Because of their narrow spectral line-widths and high energy density it is possible to excite individual electronic transitions of the target molecule without adding too much spurious energy to the system. Also, the small focal volume achievable by the focused laser beam ($\frac{\lambda}{4}$) results in high spatial resolution of the laser-particle interaction volume allowing the possibility of imaging.

The LIF technique generates a signal which is detected above a background which, under the best circumstances, is nearly zero and single-photon detection is possible. As in absorption techniques, LIF also takes advantage of the unique absorption spectrum of a molecule to achieve analyte selectivity. In this regard, LIF is also more advantageous because although some molecules may share molecular transitions, fewer molecules will subsequently fluoresce. Thus, LIF is a highly selective technique. Still, if sufficient photons are to be absorbed by the target species, a wavelength should be chosen which corresponds to a large absorption cross section for the target species and small ones for other non-fluorescing molecules which may be present.

In its simplest form, LIF for a two level system involves two steps. First, the molecule is resonantly stimulated by the absorption of a photon with energy hν. Secondly, the molecule is either radiatively or non-radiatively

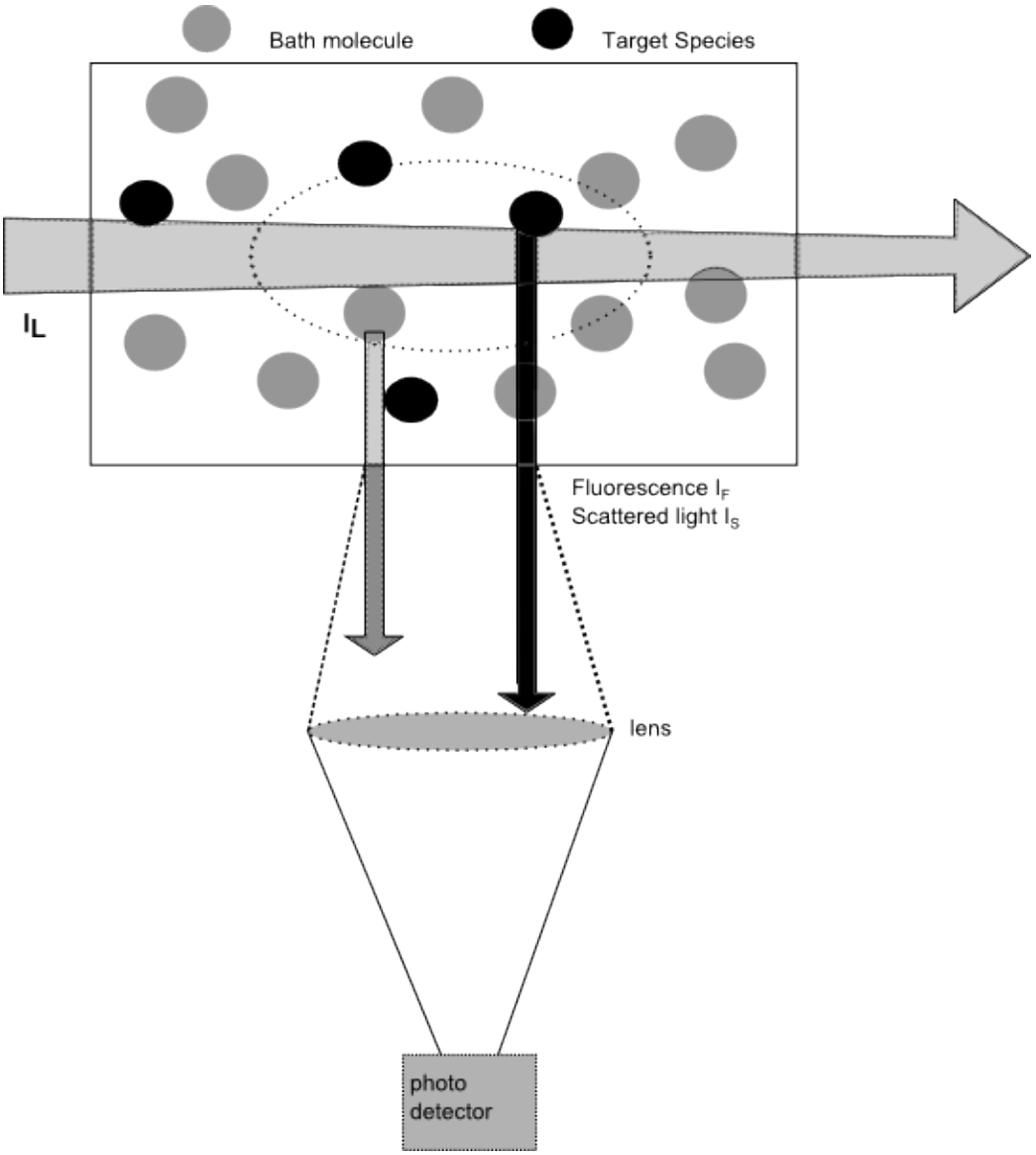

Figure 2.1: Basic Laser Induced Fluorescence setup. Fluorescence emission (I_F) from molecules in a gas mixture, after absorption of laser light I_L. Scattered laser light I_S also arrives at the detector and is a source of noise.

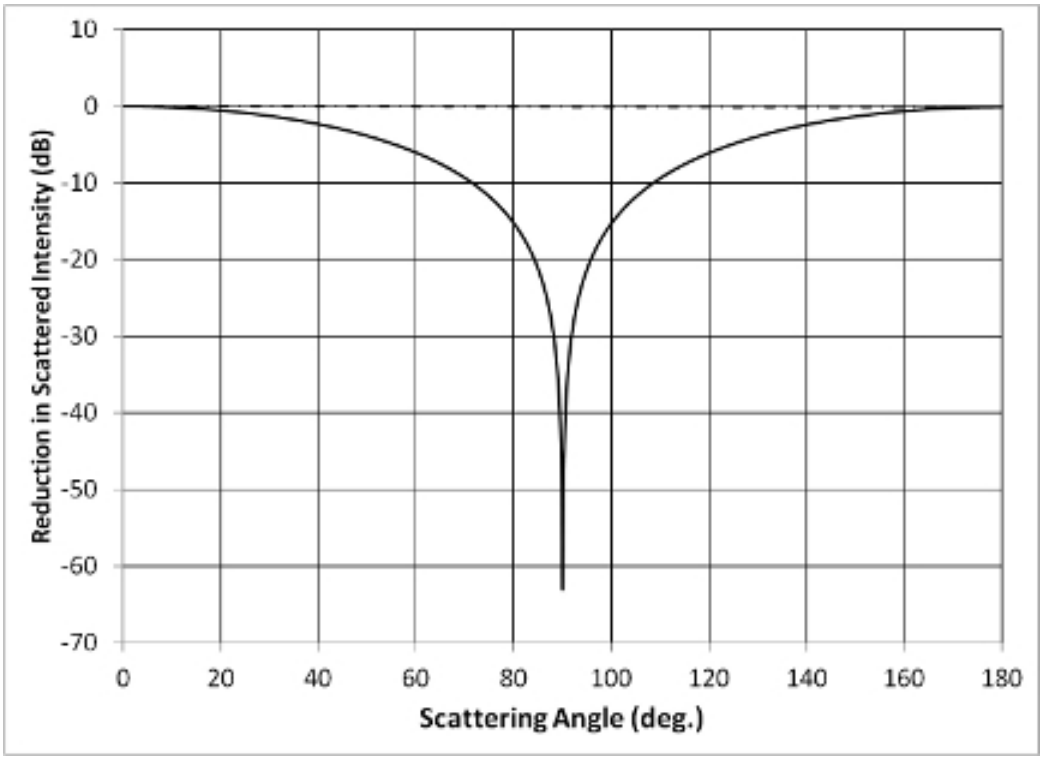

Figure 2.2: Intensity due to Rayleigh scattering in air(STP) versus scattering angle for 410 nm light, perpendicularly (dashed) and parallel (solid) polarized light to the plane of the detector.

deactivated. In the radiative deactivation the excited molecule will spontaneously emit a photon with energy equal to or less than the excitation photon. In the nonradiative quenching process the excited molecule loses its energy to 'bath' molecules. These two processes are given respectively by:

$$X^* \xrightarrow{k_r} X + h\nu \tag{2.1}$$

$$X^* + M \xrightarrow{k_q} X + M, \tag{2.2}$$

where k_r (molecules s^{-1}) is the the radiative rate constant for fluorescence, k_q (molecules s^{-1}) is the quenching rate constant of the emitting state and M is the concentration of the quencher. The effect of the two processes is that the excited molecule has a finite radiative lifetime, τ, given by:

$$\tau = \frac{1}{(k_r + k_q M)}. \tag{2.3}$$

The radiative lifetime determines how much of the potential fluorescence signal is quenched by bath molecules and therefore does not fluoresce. The remainder of the excited molecules will fluoresce giving rise to the expression for fluorescence yield of photons (FYP):

$$FYP = \frac{k_r}{(k_r + k_q M)} \times X^* \tag{2.4}$$

Because we are here dealing with gas-phase systems, pressure and concentration of bath molecules are directly proportional. Figure 2.3 shows the

pressure dependence of excited state lifetime and FYP for the system developed in chapter 3.

2.1.1 FAGE LIF technique

Under the condition that $k_q M << k_r$, which is the case when the pressure is reduced, i.e., M is reduced, equation 2.4 can be rewritten as:

$$FYP = X^*. \tag{2.5}$$

In this case the fluorescence yield is 100% of the excited molecules. By reducing the pressure, the radiative lifetime of the excited molecule is made longer, i.e., fluorescence will continue for a longer time. This increase is useful when considering noise reduction. The gross signal arriving at the detector is the sum of the analyte fluorescence and the background 'noise' due to scattered excitation photons and 'dark counts' of the detector. The scattering of excitation photons is due to Rayleigh scattering and by reflections off the optical components and walls of the instrument. Rayleigh scattering is an elastic process; meaning that when the light source is shut off, the presence of scattered photons vanishes nearly instantaneously. Because of this, the elongated lifetime of the fluorescence signal allows for temporal filtering, a noise filtering technique unique to LIF. In order to achieve temporal filtering the detector is either blocked or shut off during the pulsed excitation of the target species. When the pulse is ended and the elastically scattered

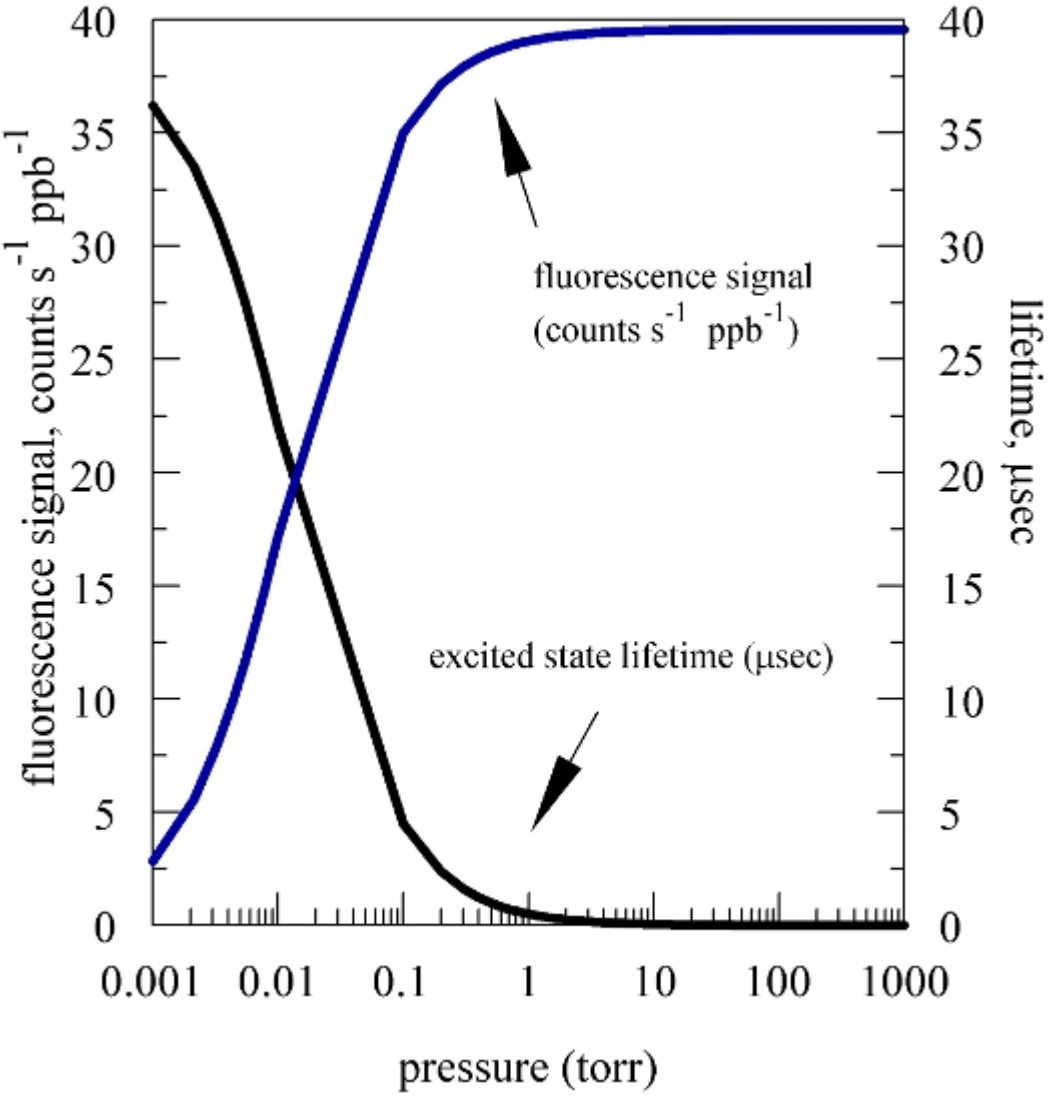

Figure 2.3: Fluorescence lifetime and yield (FYP) versus pressure. The parameters used here are those for the system developed in chapter 3: the excitation wavelength ($\lambda = 406.3$ nm), the detection solid angle ($\omega = 0.038$), the fraction of fluorescence in the PMT spectral window (F = 0.7), the transmission of the optics (0.8), the path length (l=1 cm), the absorption cross section (σ = 6 x 10^{19} cm^2 molecule^{-1}), the radiative rate constant ($k_r = \frac{1}{\tau_0}$ = 2.6 x 10^4 s^{-1}), and the quenching constant(Q = 6 x 10^{11} cm^3 molecule^{-1} s^1).

excitation photons are gone, the detector is turned on and subsequently only the fluorescence photons are detected. Temporal filtering can only work if the fluorescence lifetime of the target species is several times longer than the elctronic gates achievable with the system. For this reason the analyte is typically sampled into a moderate vaccuum ($\sim$ 1 torr) where the radiative lieftime is elongated. This technique is known as Fluorescence Assay by Gas Expansion (FAGE) (George and O'Brien, 1991; Hard et al., 1984). In this case the SNR is theoretically infinite, although imperfections in the setup cause this to not be the case. A second and useful effect of operating at lower pressure is that Rayleigh scattering, which is proportional to pressure, is reduced. This is important since in any 'real' application of FAGE, the laser cannot be shut off immediately, and so it is inevitable that some noise will be present. In the case of reduced Rayleigh scattering the noise is also reduced. Several research groups have successfully implemented LIF for in situ atmospheric measurements of NO_2 using the FAGE technique which utilizes the relatively long radiative lifetime of NO_2 at low pressures ($\sim$100 μs at 35 mtorr and 585 nm excitation) and have achieved excellent sensitivity at short averaging times.

2.2 Atmospheric Pressure LIF

Operating LIF at low pressure is not always desirable or economical. Although laser diodes have dramatically reduced the cost and energy requirements of FAGE systems (Taketani et al., 2007), the low-pressure regime of

these systems adds significant cost, energy use, and bulk via their pumping systems. For some systems under study a low pressure environment is not possible, e.g., combustion and flame studies (Barnes and Kircher, 1978; Mann et al., 1996), studying biological systems (Teklemariam and Sparks, 2006) or kinetic experiments with direct comparison to atmospheric conditions(Ramazan et al., 2006).

For most molecules an LIF system which operates at or above ambient pressures will not be able to take advantage of the elongated lifetime (cf. Figure 2.3) because the lifetime at ambient pressure is too short for readily available electronics to perform temporal filtering. In this case, low limits of detection are achieved primarily through a reduction of background noise with optical long-pass filters and by increasing the signal using higher laser powers (Barnes and Kircher, 1978; Mann et al., 1996; Parra and George, 2009). In the case of a continuous wave (CW) setup the limit of detection (LOD) for the AP-LIF system can be calculated by:

$$LOD = n\sigma, \tag{2.6}$$

where σ is the standard deviation of the signal(photons s^{-1}) distribution, and n is the number of standard deviations of separation from required at given confidence interval (e.g. n = 3 for the 1% C.I.). The gross signal is the sum of the fluorescence (S) and the background photons (B). When the noise of the gross signal is described by a Poisson distribution, as in the case

of photon counting schemes typically used for LIF, the noise (σ) associated with the signal is the sqaure root of the gross signal:

$$\sigma = \sqrt{S + 2B}. \tag{2.7}$$

To make theoretical calculations of the LOD in terms of the lowest distinguishable concentration of analyte we can use the following equation for the fluorescence signal rate:

$$S_X = C_X \times E_X \times FYP, \tag{2.8}$$

where C_X is the collection efficiency of the detection system, E_X is the excitation rate, and FYP is the fluorescence yield. Under the high pressure conditions condition that $k_q M >> k_r$ in equation 2.4 it can be written as:

$$FYP = \frac{k_r}{k_q M_q)} \times X^*. \tag{2.9}$$

In this case case X^* combines with M in the denominator as the mixing ratio of excited molecules, with the result that the number of fluorescence photons is independent of pressure (or quencher concentration) and is linearly dependent on the mixing ratio of the excited target species (cf. Figure 2.3). In this pressure regime the fluorescence yield is greatest although the fluorescence lifetime is the shortest and Rayleigh scattering will also be greater.

The fluorescing molecule will emit photons uniformly in $4 \times \pi$ steradians

of the sphere, but only a fraction of that light falls within the solid angle of the collection optics and the spectral window of a typical detector. C_X represents the efficiency involved with collecting the fluorescence signal,

$$C_X = \Omega \times F \times T, \tag{2.10}$$

where Ω is the solid angle intercepted by the collection optics for a typical off-axis design, F is the fraction of fluorescence occurring within the spectral window of the detector and T is the fraction of transmitted fluorescence through the optics (lens and filters).

E_x represents the overlap of the laser line (φ) and the wavelength dependent absorption cross section for the target molecule (σ_X). E_X has units of photons molecule^{-1}s^{-1}, and is expressed by:

$$E_X = \int \varphi(\nu)\sigma_X(\nu, temp, pressure)d\nu, \tag{2.11}$$

The SNR is proportional to the signal rate and inversely proportional to the square root of σ:

$$SNR = \frac{S}{\sigma} \tag{2.12}$$

While both the signal and noise will increase linearly with laser power (noise due to Rayleigh and wall scattering), because of σ increase, the overall SNR for atmospheric pressure LIF system will increase with laser power.

2.3 Application of AP-LIF to NO_2

Nitrogen dioxide absorbs in the UV and visible portions of the electromagnetic spectrum (Schneider et al., 1987), with largely a continuum absorption spectrum(Figure 2.4). NO_2 is also spectroscopically complex, leading to long lifetimes($\sim$100 μs) for most fluorescence transitions (Donnelly and Kaufman, 1978). The zero-pressure fluorescence lifetime, τ, and the radiative rate constant are reciprocal (equation 2.3 with M=0). Therefore a fluorescence transition with a shorter lifetime has a faster radiative rate constant and a greater fluorescence yield (equation 2.9). Shorter transitions are not advantageous in FAGE systems because of the difficulty in separating very short fluorescence signal from instantaneous scattered signal.

The fluorescence lifetime was found to be in the range of 28 to 42 μs for the 400-410 nm range (Sivakumaran et al., 2001a,b) as opposed to >80 μs for wavelengths used in other LIF instrumentation, thereby gaining a factor of 2 in fluorescence yield by exciting in the blue. Furthermore, it is advantageous to choose a wavelength further into the blue which allows more of the red-shifted fluorescence to be within the spectral window of a typical detector (200-900 nm). Table 2.1 shows a comparison of LIF instrumentation including, the excitation wavelength, the operating pressure and the limit of detection LOD. These systems, except those of Barnes and Kircher (1978), Mann et al. (1996), and this study, all operate at pressures lower than 10 Torr.

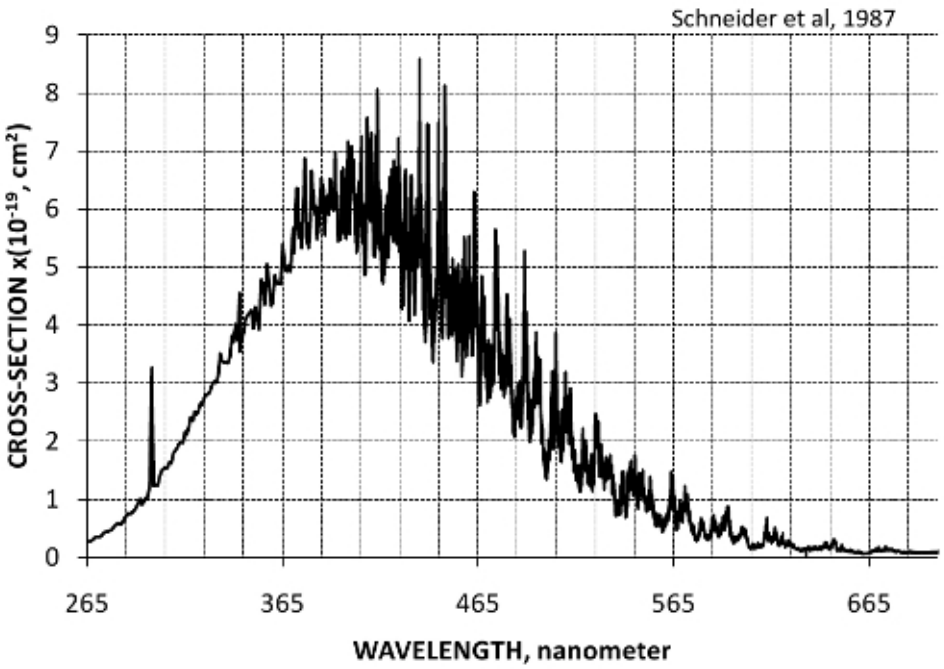

Figure 2.4: NO_2 absorption spectrum.

Table 2.1: Various LIF instrumentation for NO_2, excitation wavelength λ, radiative lifetime for the transition, operational cell pressure, and limit of detection for a 60 sec averaging interval

Reference	Excitation λ (nm)	Radiative lifetime (μs)	Cell Pressure (torr)	LOD (ppt min^{-1})
Low Pressure				
(George and O'Brien, 1991)	532	140	0.26	600
(Fong and Brune, 1997)	565	140	7.5	460
(Thornton et al., 2000)	585	100	0.35	5
(Matsumi et al., 2001)	523.5	82	0.7	125
(Cleary et al., 2002)	640.2	330	0.2	145
(Taketani et al., 2007)	473	108	0.5	140
(Taketani et al., 2007)	410	39.9[a]	0.5	390
High Pressure				
(Barnes and Kircher, 1978)	450-470	∼100	1-760	>100,000
(Mann et al., 1996)	450-480	∼ 100	760	>100,000
(Parra and George, 2009)	406.3	39[a]	760	2000

[a](Sivakumaran et al., 2001a)

The analysis above indicates that the fluorescence yield is higher at atmospheric pressure, is pressure independent, and the yield is even higher for transitions that have short lifetimes.

In order to reduce the background to make atmospheric pressure LIF measurement possible optical filters are required. Emission of the excited state is allowable to all lower lying energy states for the excited molecule, this means that fluorescence will typically be broadband and to the side of longer wavelengths (or redshifted) than that of the excitation source. For this reason a long pass (LP) optical filter is used in front of the detector.

Chapter 3

DESCRIPTION OF AP-LIF FOR AMBIENT NO_2 MONITORING

3.1 Introduction

In order to make ambient measurements with less complexity and cost, a continuous-wave laser-diode LIF-based approach for ambient measurements of NO_2 that operates at ambient pressure was developed (Parra and George, 2009). The current system has achieved sensitivity several orders of magnitude beyond previous efforts (Barnes and Kircher, 1978; Mann et al., 1996), and with further equipment improvements it promises to be a sensitive, portable, and relatively low-cost NO_2 monitoring system. The use of high-quality optical filters has facilitated low-concentration detection by providing substantial discrimination against scattered laser photons without the use of time-gated electronics, which add complexity and cost to the LIF instrumentation. This improvement allows operation at atmospheric pressure with a low-cost diaphragm sampling pump. With improvements in the optical train, it is expected that this system will easily achieve sub-parts-per-billion

detection limits, making it suitable for ambient regulatory measurements of NO_2.

3.2 Description of Ambient Monitor

The instrumental design used for the AP-LIF is typical of LIF instrumentation.The AP-LIF cell is an anodized aluminum chamber consisting of a cubic portion (4 x 4 x 4 cm) and two side arms (20 cm) ending with windows held at Brewster's angle (Figure 3.3). The overall length of the cell is thus 44 cm. A 25 mm achromatic lens with anti-reflection coating and 30 mm focal length (Edmund Optics, ACH 25 x 30 VIS-NIR) was used to collect and collimate the fluorescence signal; the focus intersected the laser line.

Based on analysis presented in chapter 2 , the expected fluorescence signal is $\sim$40 counts $s^{-1}ppb^{-1}$ for this system. To achieve a LOD of 1 ppb NO_2 for a 60 s averaging time and a SNR =2, the background should be less than 24,000 counts s^{-1}. Background reduction ($S_{bg} \approx$ 10,000 counts s^{-1}) was achieved through the use of high-quality long-pass filters. The collimated signal was passed through four long-pass filters with cut-on wavelengths at 440nm(Chroma Tech, HQ440LP) to reject scattered laser photons and transmit fluorescence photons. These filters each achieve an optical density of 5 for wavelengths shorter than 431 nm and a transmittance greater than 90% for wavelengths in the range of 448–900 nm (Figure 3.2). A second 25 mm achromatic lens with anti-reflection coating and 30 mm focal was placed after the long-pass filters and focused the signal onto the detector.

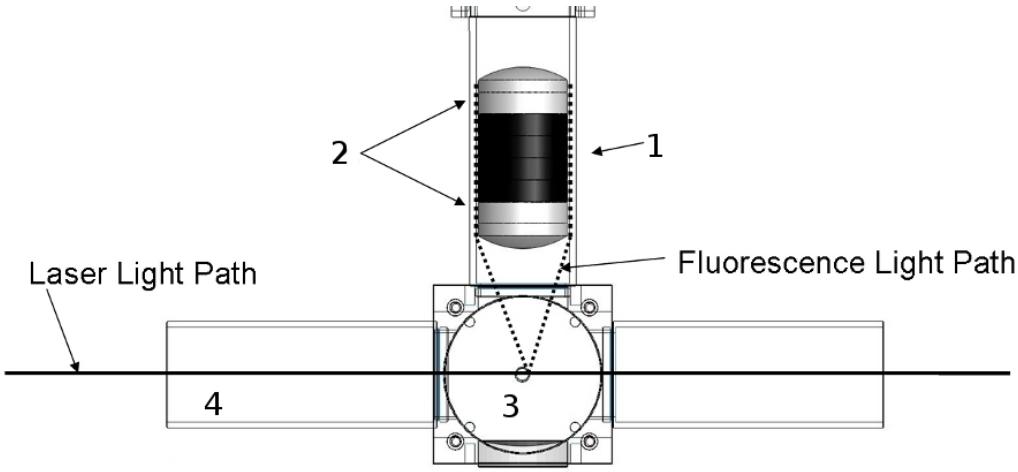

Figure 3.1: AP-LIF detection cell: 1) long-pass optical filters 2) achromatic focusing lenses 3)concave mirror 4) cell sidearms (not shown are optical baffles and Brewster angled windows.)

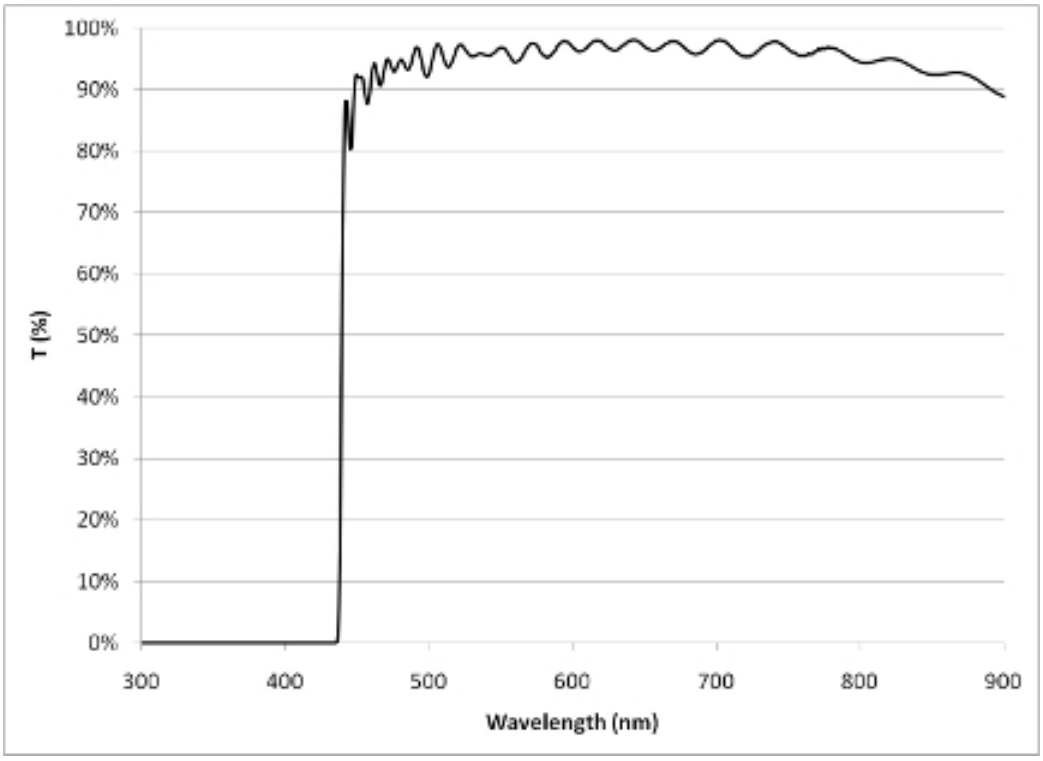

Figure 3.2: Transmission spectrum of Long Pass filters. Filters are from Chroma Tech., HQ440LP

An excitation laser beam was directed through the first window, down the length of the chamber and exited through the second window. In order to facilitate alignment of the laser beam and the detection focal volume (i.e. the center of the chamber) two 'steering' mirrors were used prior to the laser beam entering the first window (sFigure 3.1). The chamber was anodized to minimize stray light from scattering into the detector and adding to the background noise. Baffling was also added down the length of the side arms. Upon exiting the chamber the laser beam was redirected by a third steering mirror and captured in a 30 W 'beam-dump'.

Fluorescence photons were detected by a photomultiplier tube (PMT) with quantum efficiency above 10% to 900nm (Burle electron tubes, C31034). The PMT was kept at -25° C in a thermoelectric cooler (EMI Gencom, FACT 50 MKIII). The signal from the PMT was picked up by a discriminator (Phillips, Model 704) with a pulse-pair resolution of 3.3 ns. Pulses from the discriminator were counted by a 100MHz counter (Tennelec,TC531). The output of the counter was read by a digital input/output module (Measurement Computing USB-DIO96/H) and then imported to a microcomputer via the USB bus. Data acquisition software written in-house using LabView simultaneously recorded photon rate and analog signals from the laser controlling system, i.e., laser power, current, and temperature.

A temperature-and current-controlled 35mW continuous-wave GaN semiconductor laser diode centered on 405nm (Sanyo, DL 5146-152) was used for the current design. The compact and relatively inexpensive laser diode is

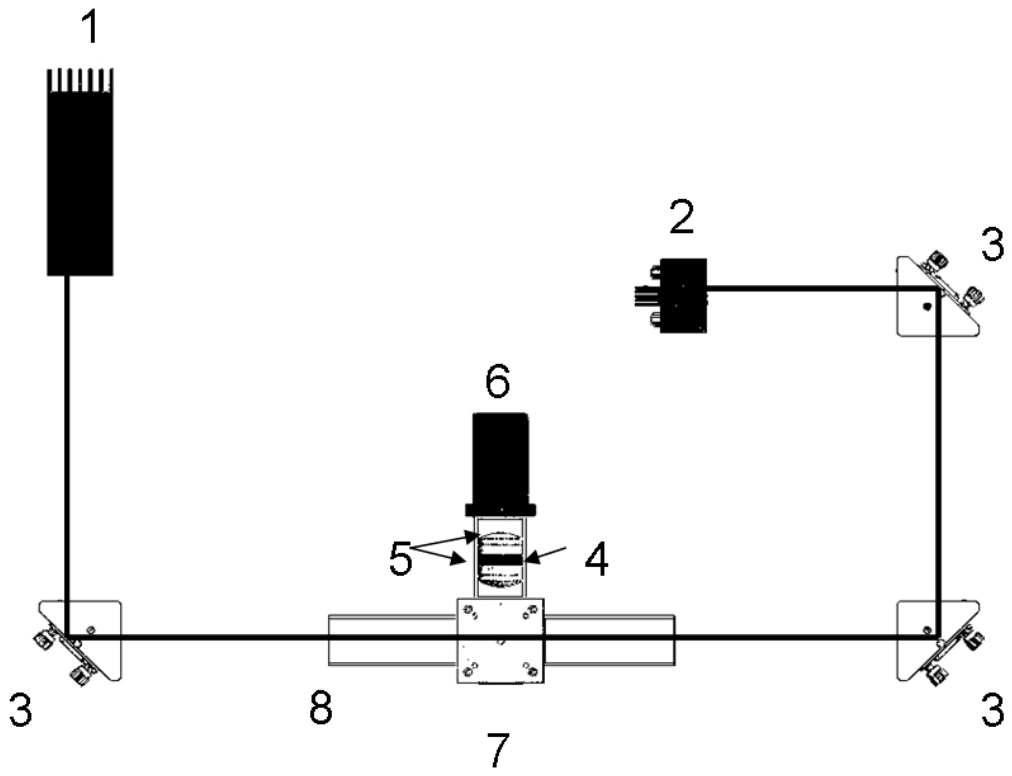

Figure 3.3: AP-LIF schematic: 1) laser source 2) laser beam dump 3) steering mirrors 4) long-pass optical filters 5) achromatic focusing lenses 6) PMT detector 7)concave mirror 8) cell sidearms (not shown are optical baffles and Brewster angled windows.)

capable of being tuned over the range of 395-415nm. Taketani et al. (2007) also employed a GaN laser diode tuned to 410nm and using the FAGE-LIF technique they were able to achieve a LOD of 390 ppt for a 60 s average time. A greater SNR was achieved by tuning the diode to 406.3 nm, where the absorption cross section of NO_2 is $\sim$6 x 10^{19}cm^{2}molecule^{-1} (Sivakumaran et al., 2001a,b) at ambient pressure and temperature. The typical lifetime for a laser diode operating near room temperature is $\sim$100,000 h.

In the two faces orthogonal to the detector and laser beam there are 0.25 in. (0.63 cm) stainless steel gas ports (Swagelok) to which 0.25in(0.63 cm) polytetrafluoroethylene tubing is connected for gas delivery and removal. Ambient measurements were made by connecting a diaphragm pump (Rietschel Thomas, Model 2107, capable of 46.1 lpm at 760 torr) to one of the gas ports while gas was drawn through the second gas port from an ambient roof-top intake manifold (Figure 3.4). Prior to entering the LIF chamber, the sample was passed through a Teflon filter (SKC, 47mm) with a 2 μm pore size to remove light-scattering particles. Background measurements (ambient air minus NO_2) were made by passing the sample through ferrous sulfate ($FeSO_4$) which reduces NO_2 to NO. A digitally controlled Teflon valve switched between ambient air and background.

Calibration of the AP-LIF instrument was performed for 0–350 ppb NO_2 concentrations. A standard of 46 $\pm$ 5 %ppm NO_2 in N_2 (Matheson Tri-Gas) was diluted with clean air using a multigas dilution system (Dasibi Model 5008). Clean air was produced from compressed ambient air passed

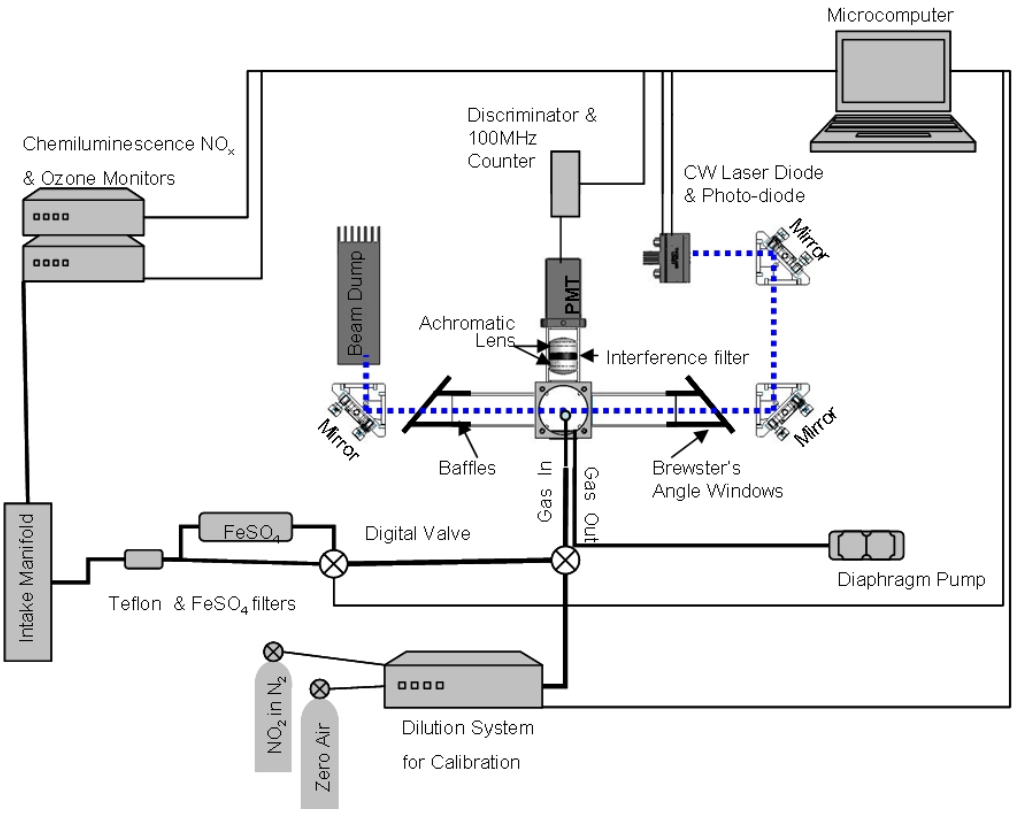

Figure 3.4: Schematic of ambient pressure LIF monitor and colocated Chemiluminescence monitor. For calibration the dilution system with NO_2 standard and zero air inputs is used to deliver various concentrations of NO_2.When monitoring ambient NO_2 the digital valve is switched to deliver the air sample through the $FeSO_4$ filter for background measurements

through a laboratory constructed Purafil/Drierite/activated charcoal/ molecular sieve filtration pack. The resulting air is ozone free, $NO_x < 1$ ppb, total volatile hydrocarbons <1 ppb, dew point -0.6 ° C. Finally, the purified air is passed through a $FeSO_4$ cartridge in order to convert residual higher oxides of nitrogen to nitric oxide. A collocated chemiluminescence NO_x (CL-NOx) (calibrated with NIST standard gases at the Oregon Department of Environmental Quality), with a stated LOD of 0.4 ppb was used for calibrating the AP-LIF instrument. Both instruments were allowed to stabilize at a given concentration for at least 30 min before using the point for calibration. The two methods are in good agreement ($r^2 = 0.998$) as shown in Figure 3.5. The slope of this plot is 16 ± 0.04 counts s^{-1} ppb−1, the standard error in y is equivalent to 2.0 ppb and the intercept is equivalent to 0.4 ± 1.6 ppb NO_2. This sets the LOD for the AP-LIF at 2 ppb (1 min averaging time), and is the lowest reported concentration LIF measurement of NO_2 at atmospheric pressure. Actual operating system parameters, such as actual optical collection efficiency, filter transmission, and overlap of fluorescence to PMT quantum efficiency, are likely to be the causes of the discrepancy between expected and achieved sensitivities. These also provide a good starting place for improving the sensitivity of the AP-LIF instrument, such as increasing the solid angle (μ) collected by adding a curved mirror opposite of the collection lens.

For ambient measurements a chemiluminescence NOx analyzer (Thermo Environ. Inc., Model 42c) and an ozone monitor (Daisibi Environ. Corp., Model 1003AH) sampled ambient air from the same manifold as the LIF

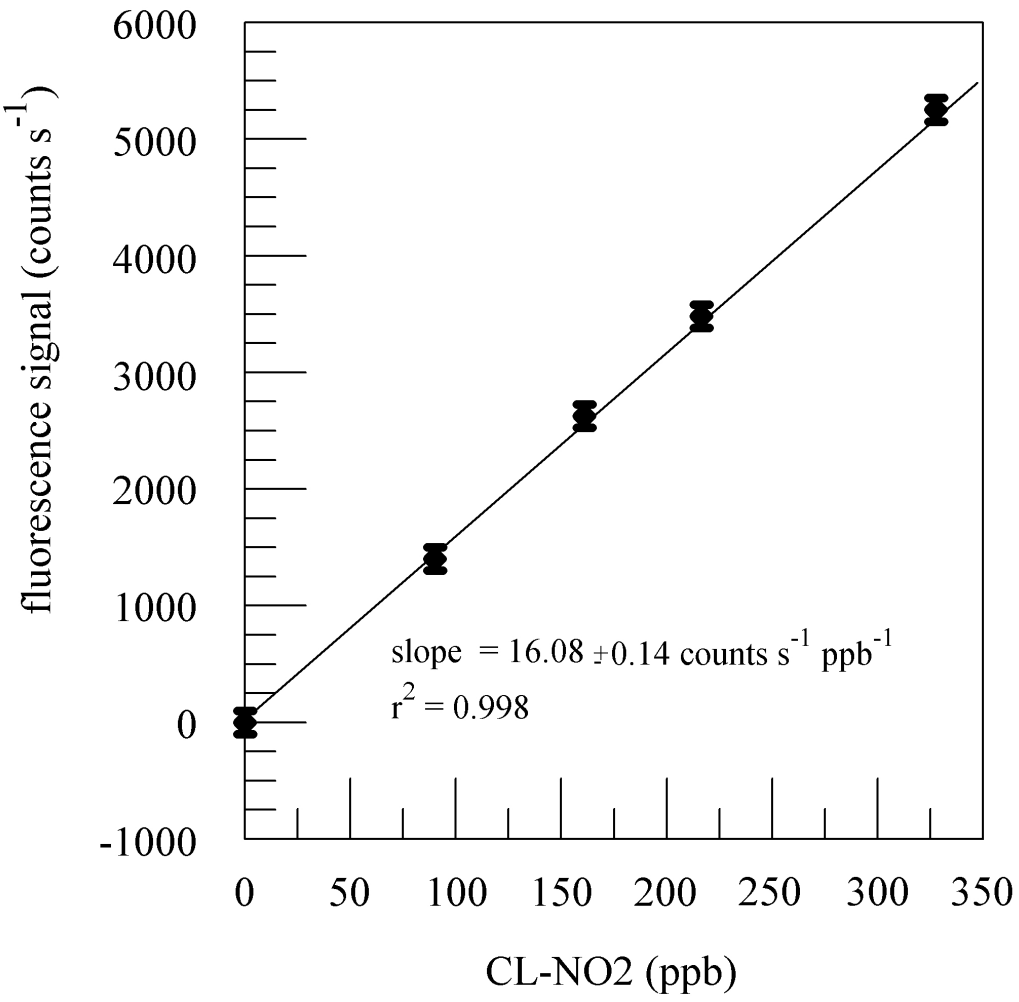

Figure 3.5: Calibration of the LIF NO_2 signal(counts s^{-1}) against a standard chemiluminescence analyzer (CL-NO_2 parts per billion).

instrument (Figure 3.4). When monitoring ambient NO_2 the digital valve is switched to deliver the air sample through the $FeSO_4$ filter for background measurements. Periodically, the AP-LIF system and CL-NOx were automatically cross compared using a dilution system to deliver a fixed NO_2 concentration followed by zero air. The data was collected by an analog-to-digital converter (Measurement Computing, USB-1408FS) and imported to the data acquisition software.

3.3 Analysis of Potential Interferences

A potential source of interference for LIF-NO_2 systems is the photolysis of ambient NO_3 to NO_2 during the time that it crosses the laser beam and the subsequent excitation to fluorescence of the produced NO_2 (George and O'Brien, 1991). For wavelengths shorter than 585nm the quantum yield of NO_2 from this reaction is near unity. The absorption cross section of NO_3 at 406.3nm is 0.2 x 10^{-19} cm^2 $molecule^{-1}$. Based on a numerical simulation of the kinetics of photodissociation, laser excitation, and fluorescence, with the flow rate and photon flux of this system the production of NO_2 from NO_3 will be negligibly low even when [NO_3] is orders of magnitude greater than [NO_2]. By operating in continuous-wave mode, this system has the advantage of very low photon density, thereby significantly reducing the likelihood of two photon inferences. Other species which can photodissociate to NO_2 include HNO_3, N_2O_5, HNO_4, peroxyacyl nitrate, and ClNOx but, with absorption cross sections 10-100,000 times smaller than that of NO_2,

these will not interfere significantly at concentrations typically found in the atmosphere. The quenching rate constant for water is 6 times greater than for air (Donnelly and Kaufman, 1978), resulting in a LIF signal reduction of ∼14% for 3% vol./vol. H_2O (approximately 100% relative humidity at 298 K) (Taketani et al., 2007). Simultaneous measurement of relative humidity and temperature can be used to correct for this when needed.

3.4 Ambient Measurements with AP-LIF

Ambient measurements of NO_2, NO, and O_3 were made 10 through 14 February 2009 at Science Building 2 on Portland State University's campus (Portland, Oregon) at a 1 min average interval. Air was drawn through a 10m long intake manifold (15 cm diameter) from the rooftop, approximately 40m above street level (the top of the intake is 2 m above the roof surface). The I-405 expressway runs 200m west and south of the building. The AP-LIF instrument, CL-NOx and ozone analyzers sampled from this manifold via 0.25 in. (0.63 cm) perfluoroalkoxy tubing. A Teflon filter with a pore size of 2 μm (SKC, 47mm) was used in front of the AP-LIF sampling tube (the same as the one integrated into the CL-NOx system). A background measurement was made once every 30 min for 5 min by passing the sample through a filter of $FeSO_4$ to convert NO_2 to NO. The ambient data is presented with a 1 min averaging time for all instruments. Figure 3.6 shows the good agreement between the two NO_2 methods (r^2 = 0.92, slope = 0.98, intercept = 0.7 ppb). It is notable that the relatively high frequency changes in NO2 levels are

reproduced by both instruments. The wind direction during this period is generally from the East with an average temperature of $\sim$5 $^{\circ}$ C; these winds originate from the Columbia River Gorge (Green et al., 2008). Nitrogen oxide and ozone anti-correlation was evident during this period. The high NO period on 12 February 2009 is attributable to the accumulation of NO emissions into the airshed during a low ventilation period (high-pressure system with very low wind speed). Since very little photochemistry was occurring during the overcast days of this period, oxidation of NO to NO_2 is limited to ozone titration.

The use of high-quality optical filters has facilitated low-concentration detection of NO_2 using AP-LIF by providing substantial discrimination against scattered laser photons without the use of time-gated electronics, which add complexity and cost to the LIF instrumentation. This improvement allows operation at atmospheric pressure with a low-cost diaphragm sampling pump.

Chemiluminescence detection of NO_2 has known and potentially significant interferences. Yet, it is the most common method for in situ ambient regulatory monitoring of NO_2. LIF offers a direct and sensitive method for ambient NO_2, but current systems are complex and costly to operate. By operating at higher pressures this system lowers the cost and complexity of LIF for in situ ambient detection of NO_2. This system can be utilized as a 'back-end' detector of an NOy ambient monitor. Since this NO_2 system does not require an expensive high-capacity pump, separate cells for each con-

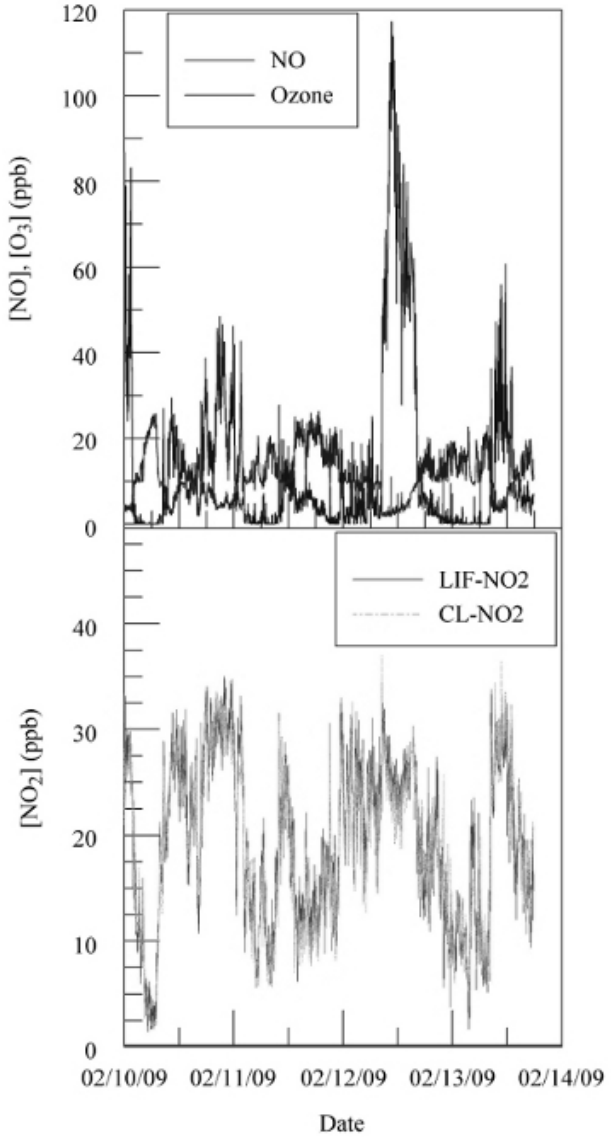

Figure 3.6: Ambient measurements of ozone, NO, CL-NO2, and AP-LIF NO_2 made 10 through 14 February 2009 at the Portland State University campus Science Building 2 near the I-405 expressway.

stituent of NOy can be employed, thereby eliminating the complexity and potential chemical artifacts associated with switching between NOy modes. In summary, the AP-LIF instrument developed here for NO_2 which may operate at atmospheric pressure has a limit of detection of 2 ppb (SNR = 2) with an averaging interval of 60 s. With improvements in the optical train, it is expected that this system could achieve sub-parts-per-billion detection limits, making it suitable for ambient measurements of NO_2. Tuning of the laser on and off the NO_2 absorption peak will eliminate the need for $FeSO_4$ for background measurements.

Chapter 4

INVESTIGATION OF HETEROGENEOUS NO_y CHEMISTRY USING AP-LIF

4.1 Introduction

The possibility that surface mediated chemistry plays a significant role in urban air chemistry has, for the past few decades, received considerable attention (Fairbrother et al., 1997; Handley et al., 2007; Kinugawa et al., 2011; Kotamarthi et al., 2001; Ramazan et al., 2004; Rivera-Figueroa et al., 2003; Saliba et al., 2001). Heterogeneous reactions have been cited for the discrepancies, up to an order of magnitude, between field measurements of nitrous acid (HONO) in the boundary layer and the known formation and destructions paths of HONO (Acker et al., 2005, 2006a,b; He et al., 2006; Kleffmann et al., 2005). While the sources of HONO are still not completely understood, in addition to direct emissions, heterogeneous pathways are the most likely source of HONO in the boundary layer (Finlayson-Pitts, 2000). Because of its importance as a daytime source of HO much research has been focused on finding plausible heterogeneous sources for HONO (Fairbrother et al., 1997;

George et al., 2005; Handley et al., 2007; Saliba et al., 2000; Ramazan et al., 2006). Up to 30 % of the boundary layer HO in the polluted environment comes from photolysis of HONO (Alicke et al., 2002). Heterogeneous hydrolysis of NO_2 (reaction R 4.1) is a significant pathway for HONO formation (Finlayson-Pitts, 2000; Finlayson-Pitts et al., 2003; Lammel and Cape, 1996; Ramazan et al., 2006).

$$2\,NO_2 + H_2O \longrightarrow HONO + HNO_3(ads) \qquad (R\,4.1)$$

In this reaction nitrous acid is released in the gas phase while nitric acid remains on the surface (Barney and Finlayson-Pitts, 2000; Goodman et al., 1999). NO_2 hydrolysis alone is not sufficient in explaining the observed nighttime build up of HONO in polluted air-masses, which is on the order of 10 ppb in polluted environments (Moussiopoulos et al., 2000). Other heterogeneous pathways have been cited as sources of HONO, such as reaction of NO_2 on suspended soot particles (Ammann et al., 1998) as well as the reaction of NO_2 with organics dissolved in aqueous solution (Gutzwiller et al., 2002). A photoenhancement of HONO generation through NO_2 hydrolysis was reported by Akimoto et al. (1987). George et al. (2005) found that photoenhanced conversion of NO_2 on organic films to produce HONO exceeds the rate of the dark reaction by an order of magnitude. Recent evidence has pointed to the possibility of HNO_3 being reduced back to photochemically active nitrogen (e.g. NO, NO_2, HONO) via surface chemistry (Ramazan

et al., 2006; Rivera-Figueroa et al., 2003; Saliba et al., 2001).

The so called 'renoxification' of surface adsorbed HNO_3 could play a significant role in urban air chemistry because of the high portion of surfaces available such as roadways, sidewalks, roofs, windows, etc. as well as high concentrations of atmospheric particles. Handley et al. (2007) found the thin films coating urban surfaces may be comprised of up to ∼7% nitrate and ∼10% organic compounds. Furthermore it was found that the existences of loss processes other than wash-off are needed to account for the measured resident lifetime of nitrate on these surfaces, pointing to heterogeneous chemistry (Handley et al., 2007).

The heterogeneous reaction of surface HNO_3 with gas-phase NO to form $HONO_{(ads)}$ and NO_2 (reaction R 4.2) was found to be thermodynamically favorable even though such a reaction in the gas phase is slow (Fairbrother et al., 1997).

$$HNO_3(ads) + NO \longrightarrow HONO(ads) + NO_2 \qquad (R\,4.2)$$

It has been suggested that reaction R 4.2 along with reaction R 4.3 represent significant pathways for returning oxides of nitrogen into the boundary layer (Ramazan et al., 2006; Rivera-Figueroa et al., 2003; Saliba et al., 2001).

$$HONO(ads) + HNO_3(ads) \longrightarrow 2\,NO_2 + H_2O \qquad (R\,4.3)$$

Renoxification of surface adsorbed HNO_3 via reaction with NO (reaction

R 4.2) has been the subject of several studies (Kaiser and Wu, 1977; Kleffmann et al., 2004; McKinnon et al., 1979; Mochida and Finlayson-Pitts, 2000; Rivera-Figueroa et al., 2003; Saliba et al., 2001; Smith, 1947; Streit et al., 1979; Svensson et al., 1987). It was reported that the reaction rate is proportional to the concentrations of HNO_3 and NO and to the surface-to-volume ratio, demonstrating the heterogeneous nature of the reaction. Saliba et al. (2001) reported that reaction depended on the amount of surface water coverage and concluded that the reaction rate reached a maximum at intermediate humidity levels corresponding to a surface water coverage of approximately three monolayers.

Several researchers have made use of FTIR to study the kinetics of renoxification under static conditions (Mochida and Finlayson-Pitts, 2000; Rivera-Figueroa et al., 2003; Saliba et al., 2001). FTIR is a desirable technique for studying heterogeneous chemistry because chemical species can be measured spectroscopically both on the surface and in the gas phase (Mochida and Finlayson-Pitts, 2000). FTIR also operates at atmospheric pressure so reaction can be studied at ambient pressure. One drawback of using FTIR to study reactions R 4.2 and R 4.3 is the high concentrations of NO_y which must be used because of the high limit of detection of FTIR ($\sim$ 1 ppm) (Mochida and Finlayson-Pitts, 2000; Rivera-Figueroa et al., 2003; Saliba et al., 2001).

For comparison the standard instrument used for ambient monitoring of NO_2 is the chemiluminescence analyzer with a typical limit of detection of $<$0.5 ppb for a 60 second average interval. Chemiluminescence is not a direct

measure of NO_2 and other NO_y under some circumstance are inadvertently measured as NO_2. suffer from interferences in studying reaction R 4.2 and R 4.3. Furthermore because chemiluminescence instruments use a detection cell held at reduced pressure (<200 torr) chemical reactions cannot be studied in situ with chemiluminescence instrumentation, instead a flow through apparatus must be used.

Kleffmann et al. (2004) using a flow through glass reactor and a chemiluminescence detector were able to use initial NO mixing ratios much closer to ambient concentrations (0.5 - 10 ppm) and concluded that under these circumstances they cocnluded that reaction R 4.2 is not a significant source of NO_2 in the atmosphere. Furthermore, the inclusion of reaction R 4.2 in field studies with low NO mixing ratios did not account for high [HONO]/[NO_2] ratio (Alicke et al., 2003; Soergel et al., 2011).

Hence, disagreement exists as to the importance of reaction R 4.2 (Kleffmann et al., 2004; Rivera-Figueroa et al., 2003; Saliba et al., 2001). Knipping and Dabdub (2002) demonstrated that the inclusion of the reaction R 4.2 in an airshed model of the South Coast Air Basin in southern California helped to resolve the long standing discrepancies between model results and observations. Their results indicate that the inclusion of reaction R 4.2 is important in correctly predicting ozone concentrations. In certain regions inclusion of this renoxification mechanism led to increases in ozone concentration as much as 30 ppb or a 20% increase over the baseline model. Rivera-Figueroa et al. (2003) found reaction R 4.2 to be of atmospheric importance, but because of

their detection method, initial mixing ratios of NO in the range from 787-5511 ppm were used. These concentrations are several orders of magnitude greater than those expected in the atmosphere. Under low NO_x conditions reaction R 4.2 was determined not to be of importance in laboratory experiments (Kleffmann et al., 2004).

Because of the disagreement about this potentially important process and the different experimental conditions under which the reactions were followed it was deemed useful make new measurements reactions R 4.2 and R 4.3 using a novel experimental setup.

In this study experiments were conducted in a static borosilicate glass reactor held at ambient pressure and relative humidities. The static reactor was coupled to an atmospheric pressure laser induced fluorimeter(AP-LIF) to detect gas-phase nitrogen dioxide. Laser induced fluorescence (LIF) is a desirable technique for this study, because it is a direct measure of NO_2 and therefore will not suffer interferences from the other NO_y species. Also, because of its operation at atmospheric pressure the AP-LIF is well suited for studying gas-phase reaction which may have different kinetics at reduced pressures. The AP-LIF instrument used here and described elsewhere was developed as an ambient NO_2 monitor (Parra and George, 2009) but was reconfigured to work as a static cell reactor for studying reactions R 4.2 and R 4.3.

Briefly, the AP-LIF uses laser light from a 410nm, 100mW, continuous wave laser diode to excite NO_2 molecules. Excited state molecules, NO_2*,

lose energy through non-radiative quenching or by fluorescing. Fluorescence light , proportional to [NO_2], is collected, filtered against excitation source photons, and subsequently detected by a photo multiplier tube (EMI, 9816) which is held orthogonal to the laser beam.

4.2 Description of Static Cell Reactor with coupled AP-LIF Detector

In order to study reactions R 4.2 and R 4.3 the AP-LIF was coupled to 1 liter spherical borosilicate glass bulb with a surface area of 483 cm^2 (Figure 4.1). The volume of the AP-LIF cell was 780 cc. The volume of the coupled system was V=1.78 liters. The surface area of the glass reactor was 0.0483 m^2. The AP-LIF chamber walls were coated with halocarbon wax (Halocarbon Products Inc. Series 1500) to prevent surface reactions from taking place on the aluminum detection cell walls. The surface to volume ratio for the coupled system was S/V = 27 m^{-1}.

The glass reactor was conditioned with nitric acid prior to experiments. This pre-conditioning was carried out with the glass reactor decoupled from the AP-LIF instrument. Dry, gaseous HNO_3 was obtained from the vapor above a HNO_3/H_2SO_4 mixture (1:2/v:v). The glass reactor was first washed with Milli-Q water (Millipore, 18 MΩ) and then pumped down to 100 mtorr while being heated for 30 minutes to remove any surface water. The glass reactor was then exposed to 30 mtorr ($\sim$1 x 10^{18} molecules) of $HNO_{3(g)}$. After exposing the reactor for 30 minutes it was again evacuated to 100

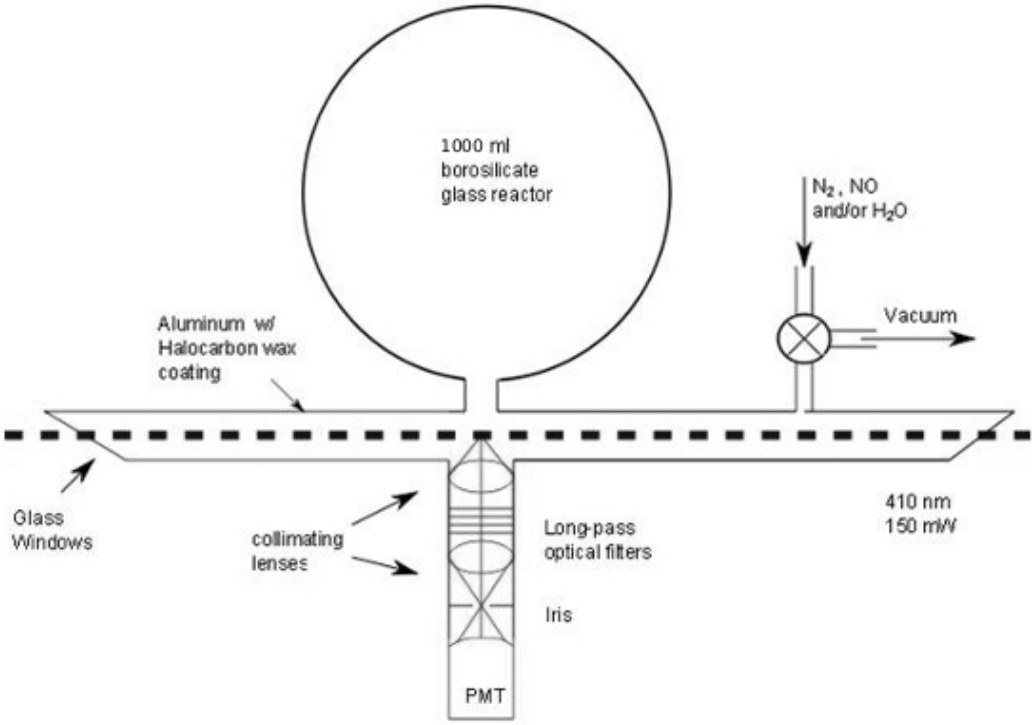

Figure 4.1: Setup for studying heterogeneous NO_2 chemistry. A 1 liter borosilicate glass reactor coupled to AP-LIF.

mtorr for 5 minutes. This procedure was repeated 3 times ending with a 30 minute pump down to get rid of gaseous oxides of nitrogen. This nitric acid 'conditioning' method was similar to that used by Saliba et al. (2001). Between experiments and prior to blank runs the glass reactor was removed from the AP-LIF, rinsed with Mill-Q water and evacuated to 100 mtorr for 30 minutes to remove water vapor and any surface contaminants. After the glass reactor had been treated it was affixed to the AP-LIF. The coupled system and the gas delivery tubing were then pumped down to 100 mtorr for at least 10 minutes before experiments.

In each experiment either 0 or 2.5 ppm of NO in N_2 was introduced into the reactor. The desired mixing ratio of NO was produced using a dilution system (Dasibi 5008) to mix a humidified N_2 stream and NO. The desired relative humidity was achieved by bubbling N_2 through Milli-Q water (Millipore, 18 MΩ). This produced a stream with 100% RH which was then diluted with dry N_2 to achieve the desired relative humidity (0-75% RH). The desired concentration of NO and RH was introduced into the reactor via 1/8" PFA tubing and a stainless steel T-piece junction at a flow rate of 1 lpm. One leg of the T-piece was able to be switched between a vacuum pump and exhaust(Figure 4.1). The other leg of the T-piece was connected to the reactor via 1/8" stainless steel tubing. A stainless steel valve situated near the reactor allowed the reactor to be isolated from the gas delivery tubing during experiments. The [NO]/RH mixture was flowed into the previously evacuated chamber until the chamber pressure was at 1 atm.

Calibration of the coupled system was carried out by first rinsing the borosilicate glass bulb with Milli-Q water and subsequently pumping on it while being heating to remove water and any other surface contaminants. The reactor was assembled and the entire reactor system was evacuated to 100 mtorr for 30 minutes to get rid of any gaseous NO_y. The reactor was filled with the desired concentration of NO_2 and the LIF signal was recorded for at least 30 minutes.

After treating the surface with nitric acid the total surface HNO_3 (measured as NO_3^-) and HONO (measured as NO_2^-) concentrations were determined using a standard NaOH titration method using bromothymol blue indicator. A diazo dye colourimetric technique was used to measure the surface adsrobed HONO alone. Sample from a 250 ml wash was reacted with sulphanilamide to form a diazo compound. The sample was then reacted with N-(1-naphthyl) ethylenediamine dihydrochloride to form an azo dye. The diazo dye intensity, proportional to the nitrite concentration, was determined colourimetrically at 520nm and compared to identically-prepared standard and blank solutions.(Zhou et al., 2011)

HNO_3 used was 70 wt % (Sigma-Aldrich) and H_2SO_4 was 95.8 wt % (Sigma-Aldrich). NO in N_2 (Airgas, 73.65 ppm) was passed through a packed $FeSO_4$ filter to reduce any higher oxides of nitrogen to NO. Nitrogen (Polar, 99.999%) was used without further purification.

4.3 Results

4.3.1 Calibration of Static Cell Reactor with coupled AP-LIF Detector

Figure 4.2 shows a calibration curve for the AP-LIF reactor. The sensitivity of this instrument is 4.5 ppb count^{-1} s, and the standard error is 4 ppb (5 min ave.) corresponding to a LOD = 38 ppb for NO_2. The low LOD allows measurements of the potential renoxification reaction for NO_2 levels expected in the urban environment (10-100 ppb).

The surface adsorbed HONO concentration was determined by a diazo dye technique with an average $[NO_2^-]$= 1.42 $\pm$ 0.38 x10^{16} molecules. Surface adsorbed HNO_3 was determined by subtracting the nitrite concentration from the total nitrate and nitrite concentration ($[NO_3^-]$ + $[NO_2^-]$) found through titration; the average nitric acid concentration was found to be $[NO_3^-]$ = 1.27 $\pm$ 0.20 x 10^{17} molecules. This corresponded to a surface coverage for HONO and HNO_3 of 2.93 x 10^{13} and 2.64 x 10^{14} molecules cm^{-2}, respectively. The fact that nitrite was found adsorbed to the reactor walls following treatment with dry gaseous nitric acid was not entirely unexpected. Handley et al. (2007) found that some of the gas-phase nitric acid taken up by organic films would yield its dissociated form (i.e., H^+ + NO_3^-). Furthermore, illumination of the film with actinic radiation caused deprotonation possibly releasing gas phase HONO and/or NO_2. Similarly, Ramazan et al. (2004) suggested that photoenhanced catalysis of HNO_3 on wet surfaces to form HONO on wet

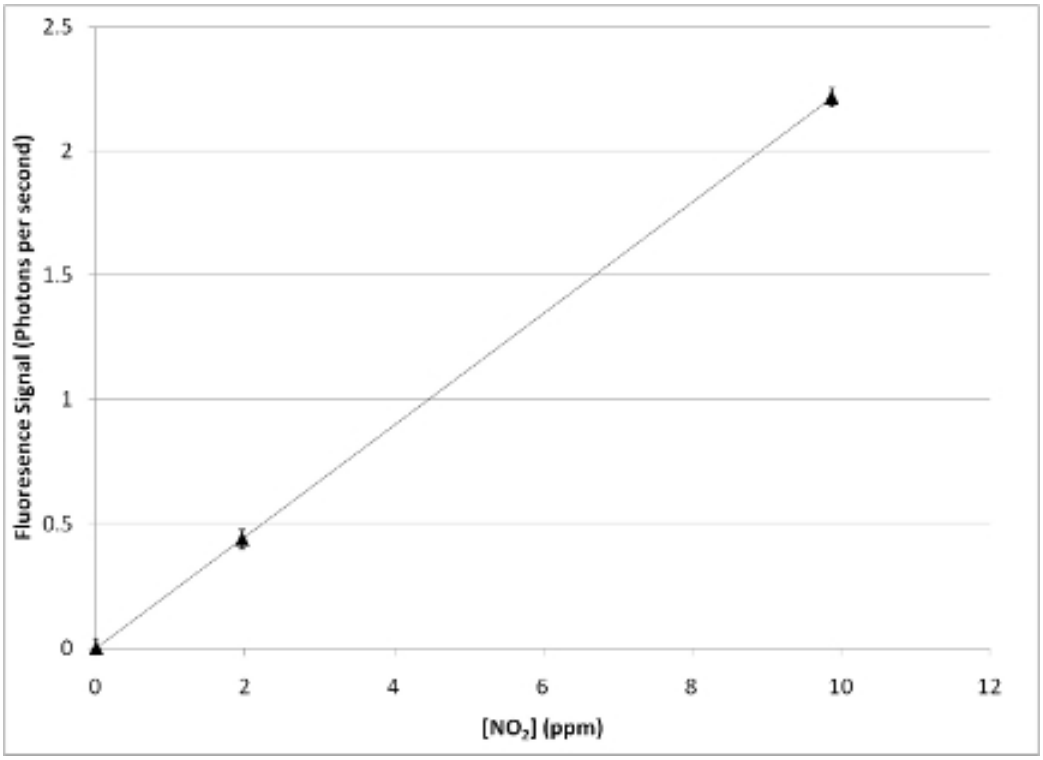

Figure 4.2: Calibration of static reactor coupled to AP-LIF detector. The LOD = 38 ppb (2 σ) at a 5 min ave. interval.

surfaces was energetically possible for wavelengths below 700nm:

$$HNO_3 + H_2O(ads) + h\nu(\lambda < 710nm) \longrightarrow HONO(ads) + H_2O(ads) \quad (R\,4.4)$$

4.3.2 Formation of NO_2 from surface adsorbed HNO_3 and HONO

Reaction R 4.3 has been found to happen much faster than reaction R 4.2 (Kleffmann et al., 2004; Mochida and Finlayson-Pitts, 2000; Rivera-Figueroa et al., 2003; Saliba et al., 2001). Kleffmann et al. (2004) found the rate of NO_2 formation by reaction R 4.3 was linear with HONO and HNO_3 concentrations as well as surface-to-volume ratio, indicating that reaction R 4.3 was indeed a surface reaction. It was seen that the rate constant of reaction R 4.3, which was independent of HONO and HNO_3 concentration, had a exponential dependence on relative humidity (k(3) = 2-15 x 10^{-17} cm^3 s^{-1} cm for 21-85% RH). Reactions R 4.3 and R 4.1 are of importance in understanding the cycling between HONO and NO_2 where there are large sources of HONO (i.e. in urban settings) (Calvert et al., 1994).

Because HONO was found adsorbed to the surface after the HNO_3 surface treatment the rate production of NO_2 via reaction R 4.2 and its dependence on the concentration of water vapor first needed to be quantified so that it could be subtracted when considering NO_2 production via reaction R 4.2. In these experiments, after being treated with dry gaseous HNO_3, the reactor was filled with N_2 (up to 1 atm) and with varying relative humidity. During the experiments significant amounts of NO_2 were formed (see Table 4.1).

Table 4.1: Initial reactant NO, RH and initial rate of NO_2 formation.

RH (%)	NO (ppbv)	dNO_2/dt (molecules cm^{-3} sec^{-1})
0	0	3.2E+05
23	0	1.3E+10
14	0	1.5E+10
28	0	3.4E+10
17	0	3.9E+10
36	0	1.2E+11
32	0	1.2E+11
66	0	1.2E+12
69	0	1.3E+12
68	0	1.4E+12
1	2455	8.0E+04
16	2455	1.2E+10
45	2455	2.2E+11
72	2455	1.3E+12

Figure 4.3 shows the time profiles of NO_2 formation at 0, 32 and 66% RH respectively. The rate of formation of NO_2 increased with RH. That the interaction is happening at the surface is further indicated by the fact that the production rate of NO_2 is not linear with water vapor. Instead the formation of NO_2 seemed to match well with the number of expected layers of water on the surface. Fractional water coverage was calculated using the equation for a BET isotherm:

$$fractional coverage = \frac{c_B RH}{(1 - RH)[1 + (c_B - 1)RH]} \tag{4.1}$$

where the constant $c_B = 100$ was used. Figure 4.4 shows the theoretical layers of water on the borosilicate glass as well as the rate of formation of NO_2 versus relative humidity. This result, that the rate of NO_2 depends on fractional water coverage, is similar to that found in other studies (Rivera-Figueroa et al., 2003; Saliba et al., 2001).

4.3.3 Formation of NO_2 from surface adsorbed HNO_3 and gas-phase NO

Reaction R 4.2 was investigated in several experiments at relative humidities in the range of 0-72% and a NO mixing ratio of 2.5 ppm. In these experiments, after being treated with dry gaseous HNO_3, the reactor was filled up to 1 atm with NO_2 in N_2 at a mixing ratio of 2.5 ppm and with varying relative humidity. Production of NO_2 did not exceed production due to

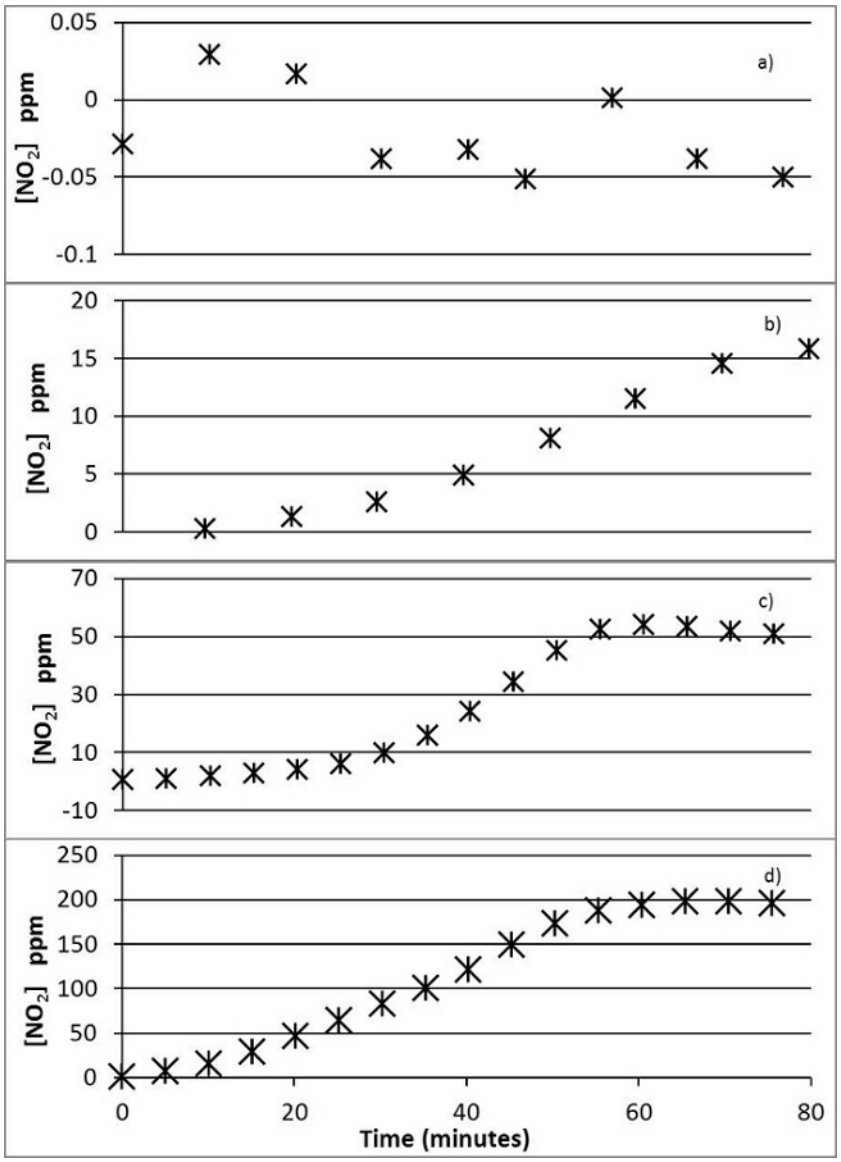

Figure 4.3: NO_2 concentration versus time for HNO_3 conditioned reactor held a different RH: a) RH = O%, b) RH = 17%, c) RH = 32%, and d) RH = 66%.

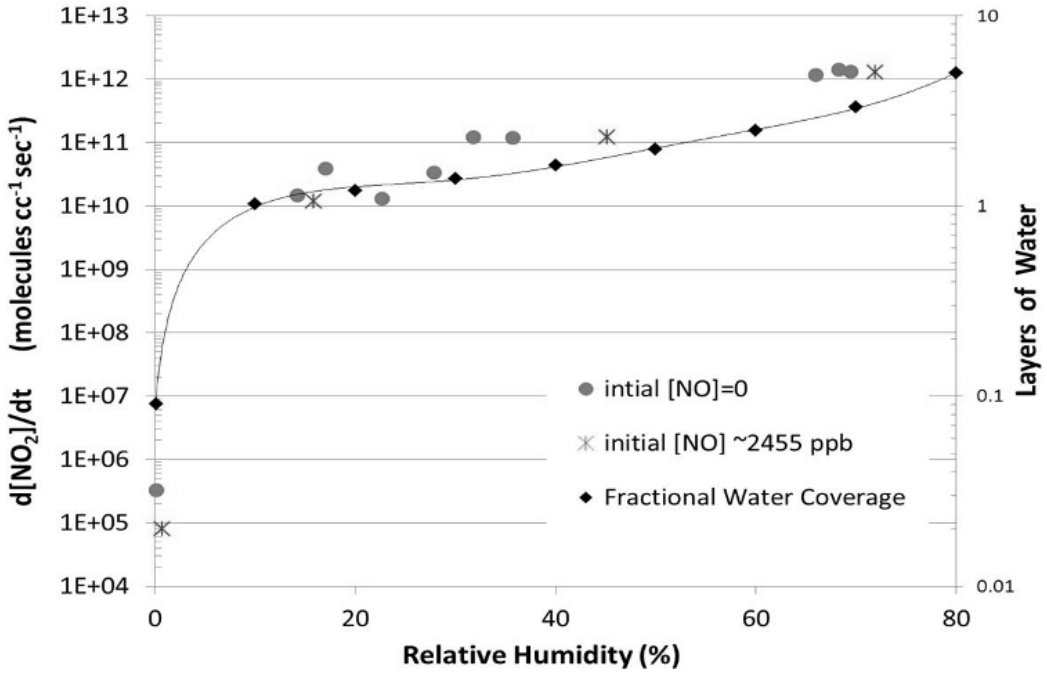

Figure 4.4: Rate of NO_2 production and surface water coverage (stars) versus relative humidity for the HNO_3 conditioned vessel. Initial NO concentration were 0 for gray circles and 2455 ppb for black circles.

reaction R 4.3. The rate of production of NO_2 due to reaction R 4.3 was subtracted from the intial reaction rates found when introducing [NO] = 2.5 ppm (Figure 4.6).

Reaction probabilities (γ) for reaction R 4.2 can be calculated. The reaction probability for NO reacting with surface adsorbed HNO_3 can be calculated using the initial loss rate of NO ($\frac{d[NO]}{dt}$), the cell volume (V_{cell}), and the surface area (A) of the reactor and M is the molecular weight of NO:

$$\gamma = \frac{(\frac{-d[NO]}{dt})V_{\text{cell}}}{A[NO]_0\sqrt{\frac{RT}{2\pi M}}}. \tag{4.2}$$

However in this case NO was not measured, instead we use a third of the initial NO_2 production rate based on the overall stoichiometry of reaction R 4.2. The upper limit for the reaction probability in these experiments was found to be $\gamma_{NO->NO_2} < 3 \pm 3$ x 10^{-9}. The greatest uncertainty was found for relative humidities greater than 70%; with the error most likely coming from the uncertainty in HONO being produced (see discussion).

There has been general disagreement as to the importance of reaction R 4.2 the renoxification of surface bound HNO_3. Using static cell conditions Rivera-Figueroa et al. (2003) set the lower limit for $\gamma_{NO->NO_2}$ at 6 ± 2 x 10^{-9} ; similarly Saliba et al. (2001) estimated $\gamma_{NO->NO_2}$ was on the order of 10^{-8} . In contrast, Kleffmann et al. (2004) set the upper limit for $\gamma_{NO->NO_2} < 2.5$ x 10^{-9}. In that study a flow through system was used, coupled to a chemiluminescence analyzer which allowed for lower NO_y concentration to

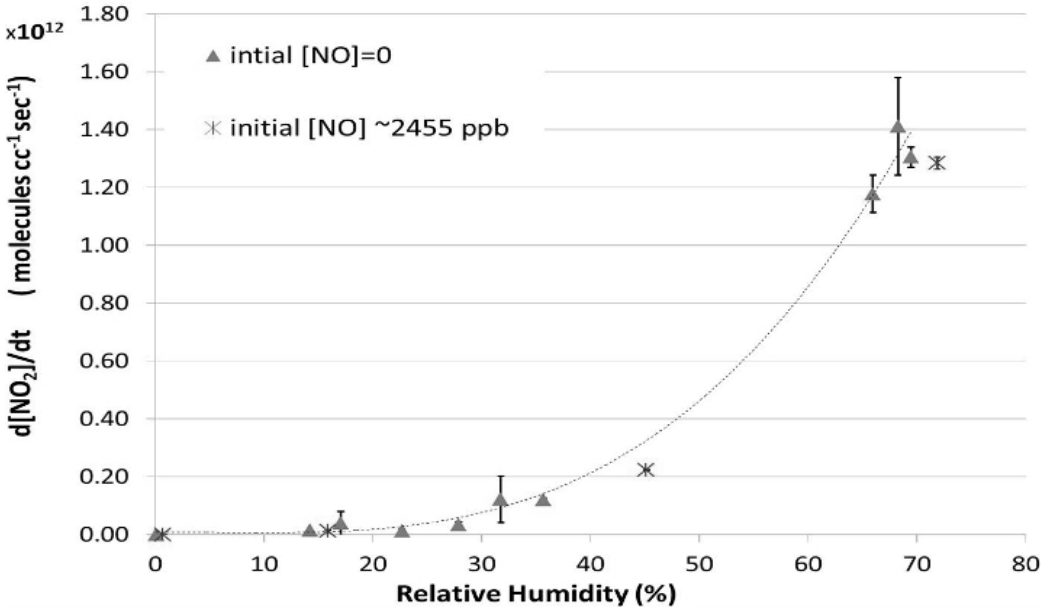

Figure 4.5: NO_2 production versus RH for HNO_3 conditioned reactor with [NO]=0 (triangles) and 2.5 ppm(stars).

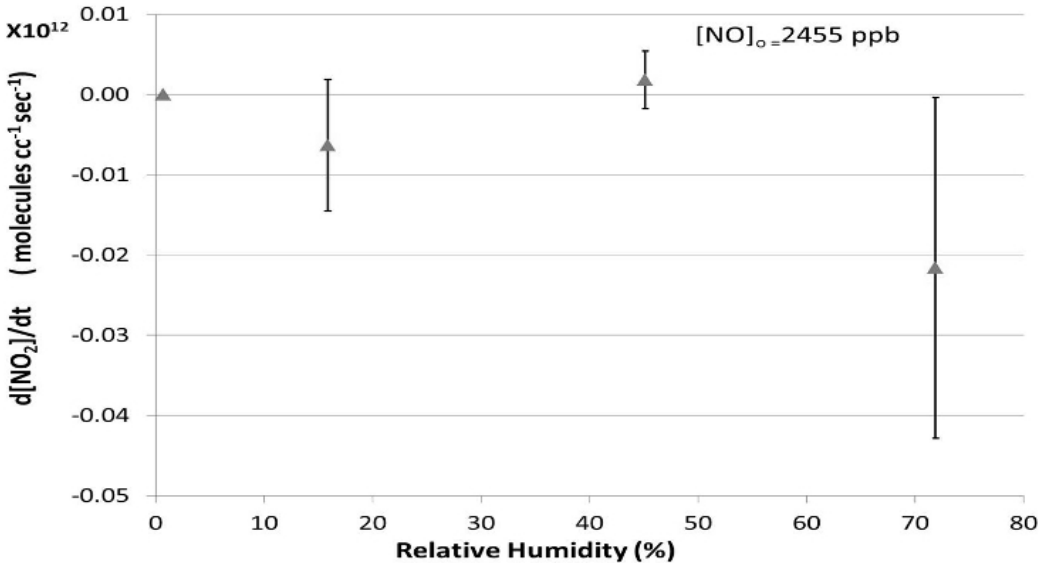

Figure 4.6: NO_2 production due to reaction R 4.3 versus RH with NO=2.5ppm.

be used.

The work done here, using the AP-LIF coupled static reactor, is in line with the results found by Kleffmann et al. (2004). The finding here set the value of $\gamma_{NO->NO_2} < 3 \pm 3$ x 10^{-9} which is considerably lower than other studies of reaction R 4.3 conducted under static cell conditions using much higher initial NO concentrations. In the case that the reaction kinetics of the urban impervious surfaces are similar to borosilicate glass, the overall reaction of nitric oxide reacting with surface bound nitric acid to form NO_2 does not appear to be of importance for atmospheric renoxification.

4.4 Discussion

Within experimental accuracy no NO_2 was seen to be produced for 0% RH. Kleffmann et al. (2004) found reaction R 4.3 to be first order in both [HONO] and [HNO_3] and that the rate constant for reaction R 4.3 was exponentially dependent on water vapor, $k(3)^{296\pm1K} = 3.39$ x 10^{-16} exp(-3.19 X 10^{-2} RH) (cm^3 s^{-1} cm) (Kleffmann et al., 2004). This being the case we should expect to see NO_2 formed even at 0% RH, given that both HNO_3 and HONO were determined to be present on the surface after rinsing. The lack of NO_2 production suggest that for our investigation HONO is not formed on the surface when water is not present. It is suspected that the surface HONO is formed after the surface comes into contact with water.

Also, since the rate constant is expected to decrease exponentially with water vapor (Kleffmann et al., 2004) and because reaction R 4.3 is first order

in [HONO] we can conclude from these experiments that as the water vapor increases more HONO is produced either in the gas phase or adsorbed to the surface.

While the glass reactor is optically isolated from the AP-LIF excitation laser (internally and externally), steps were taken to verify that surface chemistry was not being photocatalyzed by the laser source. This was accomplished by allowing reaction R 4.3 to take place with the AP-LIF laser turned off and only turned on briefly every ten minutes for 30 seconds to get a measure of [NO_2]. The rate of NO_2 production under these conditions was the same as that found with the AP-LIF laser source on all the time (see Table 4.1). Other sources for the generation of surface adsorbed HONO may exists, and there is strong evidence in field studies that there are indeed non-photochemical heterogeneous sources of HONO yet to be identified (Ziemba et al., 2010). It may be the case that the formation of surface HONO from HNO_3 adsorbed on wet glass like surfaces could account for some of this missing source. Further investigations of HONO production via this pathway are needed.

AP-LIF has proven adaptable to the study of in situ measurement of heterogeneous chemistry under more 'real' environmental conditions. A future experimental setup will take advantage of some of the improvements to reduce the limit of detection. Furthermore, AP-LIF for NO_2 could be used in tandem with FTIR so that more species may be followed while providing a greater sensitivity for NO_2.

Chapter 5

Further Work with AP-LIF

5.1 Thermal dissociation AP-LIF for measurement of NO_y

As with all NO2-LIF systems this system can be utilized as a 'back-end' detector of an NO_y ambient monitor. The term NO_y is used to denote the sum of all nitrogen compounds in air, i.e., $NO_y = NO_x + PAN + HNO_3 + NO_3^-$(Particulate) + $2\,N_2O_5$ + Other reactive N compounds. Because some of these species can be long lived in the atmosphere, monitoring NO_y is critical for understanding how oxides of nitrogen are transported to remote areas. The low pressure LIF technique coupled to a thermal dissociation (TD-LIF) oven has been successfully used to measure atmospheric NO_y (Day et al., 2002). When heated most NO_y species will dissociate into NO_2 and a companion radical species

$$XNO_2 + \text{heat} \longrightarrow x + NO_2 \qquad \text{(R 5.1)}$$

where x = RO_2, RC(O)OO, RO, OH, HO_2, NO_3, ClO, BrO. With different NO_y species dissociating at different temperatures a TD-LIF instrument can be built with multiple ovens to selectively dissociate and measure individual groups of oxides of nitrogen (Day et al., 2002)

Separate detection cells for each constituent of NO_y are employed eliminating the complexity and potential chemical artifacts associated with switching between NO_y modes (Day et al., 2002). Figure 5.1 illustrates a conceptual schematic of the AP-LIF for NO_2 , peroxyacyl nitrates (PAN) , alkyl nitrates (AN), nitric acid.

Laser light is directed by steering mirrors sequentially through the four cells and into beam dump. The fluorescence light signals are collected at each fluorescence cell with respective fiber collection optics to fiber optic multiplexer (Figure 5.2) and then into filter pack which contains a pair of lenses and a long pass filter. The signal from filter pack is then detected by PMT and processed. Inside the housing of the multiplexer is a right prism with a mirrored surface on the hypotenuse. The face of the mirror is at 45 degrees to the end of the cylindrical housing. A stepper motor is attached to the right prism through one end of the housing. The positions of the fiber optic ports correspond to the positions of the stepper motor such that, for each position of the mirror, the light entering from one of the fibers is reflected off the mirror and directed out of the end of the housing. It then passes through the filter pack and into the PMT. Using this multiplexer, the signals coming from the four fluorescence cells may be sampled sequentially as the

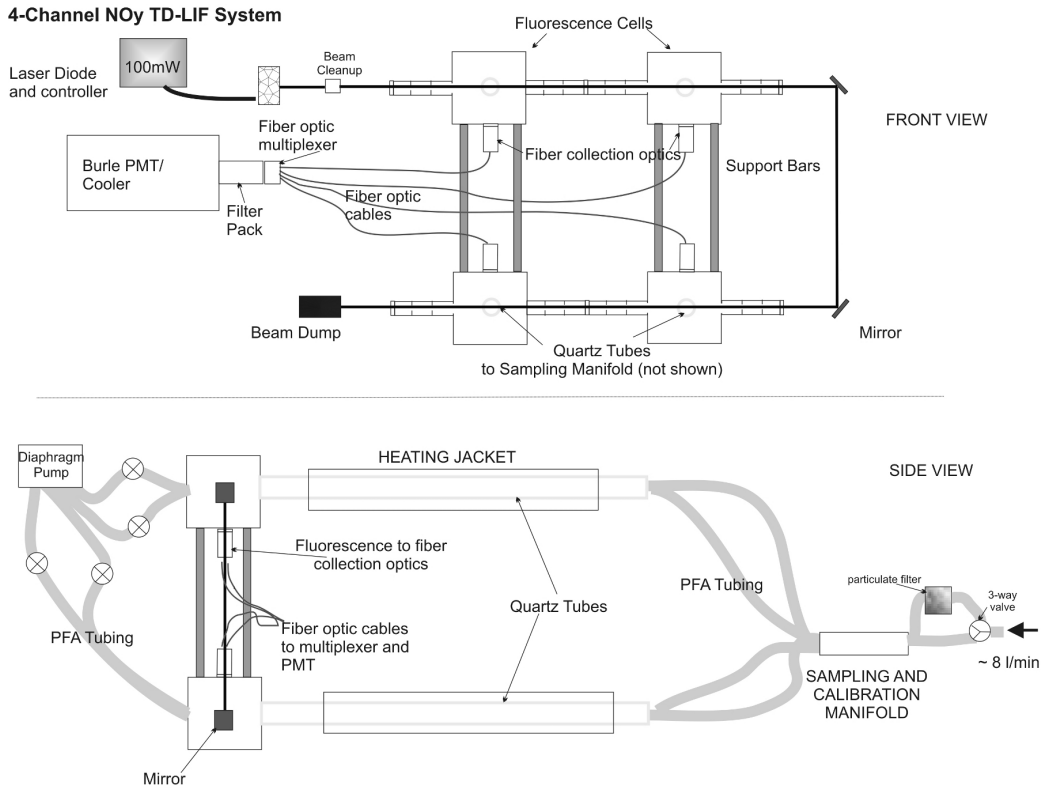

Figure 5.1: Conceptual schematic of a thermal dissociation AP-LIF instrument for NO_2, PAN, AN and HNO_3 with ovens held at ambient temp., 200° C, 400° C, 600° C, respectively.

mirror rotates using just a single filter pack and PMT. This design eliminates the cost, bulk, complexity and power requirements of 3 PMT/cooler systems and also minimizes the need for cross-channel calibrations in order to account for differences such as PMT quantum efficiencies and photon counting electronics. A diaphragm pump can be used to draw ambient gas for sampling into the four cells through four respective gas flow tubes originating from a common sampling and calibration manifold and particulate filter. The separate tubes have respective quartz tube sections which may be heated to distinct predetermined temperatures. These quartz thermal dissociation flow tubes ($\sim$ 1 m length, 1 cm ID) are coupled to each of the four cells. Three flow tubes are temperature controlled at approximately 200° C, 400° C, 600° C, respectively for thermal dissociation of PAN, AN and HNO_3 measurements respectively, using nichrome wire heating jackets and a custom-built controller circuit (Day et al., 2002). Each subsequently hotter oven thermally dissociates the species which require lower temperature to be converted to NO_2. Thus, to get [NO_3] the AN channel must be subtracted from the HNO_3 channel. The fourth tube, for ambient NO_2 measurement, is insulated but not heated. Thus, each of the three distinct species of interest may be detected by converting it by heat to NO_2 which is then measured to derive the amount of the original species of interest. Particulate nitrate (PN) can also be measured by recording the difference in the NO3 channel (i.e. 600° C oven) with and without the particulate filter in place. Since this NO_2 detection technique does not require an expensive high-capacity

pump, separate cells for each constituent of NO_y can be employed, thereby eliminating the complexity and potential chemical artifacts associated with switching between NO_y modes.

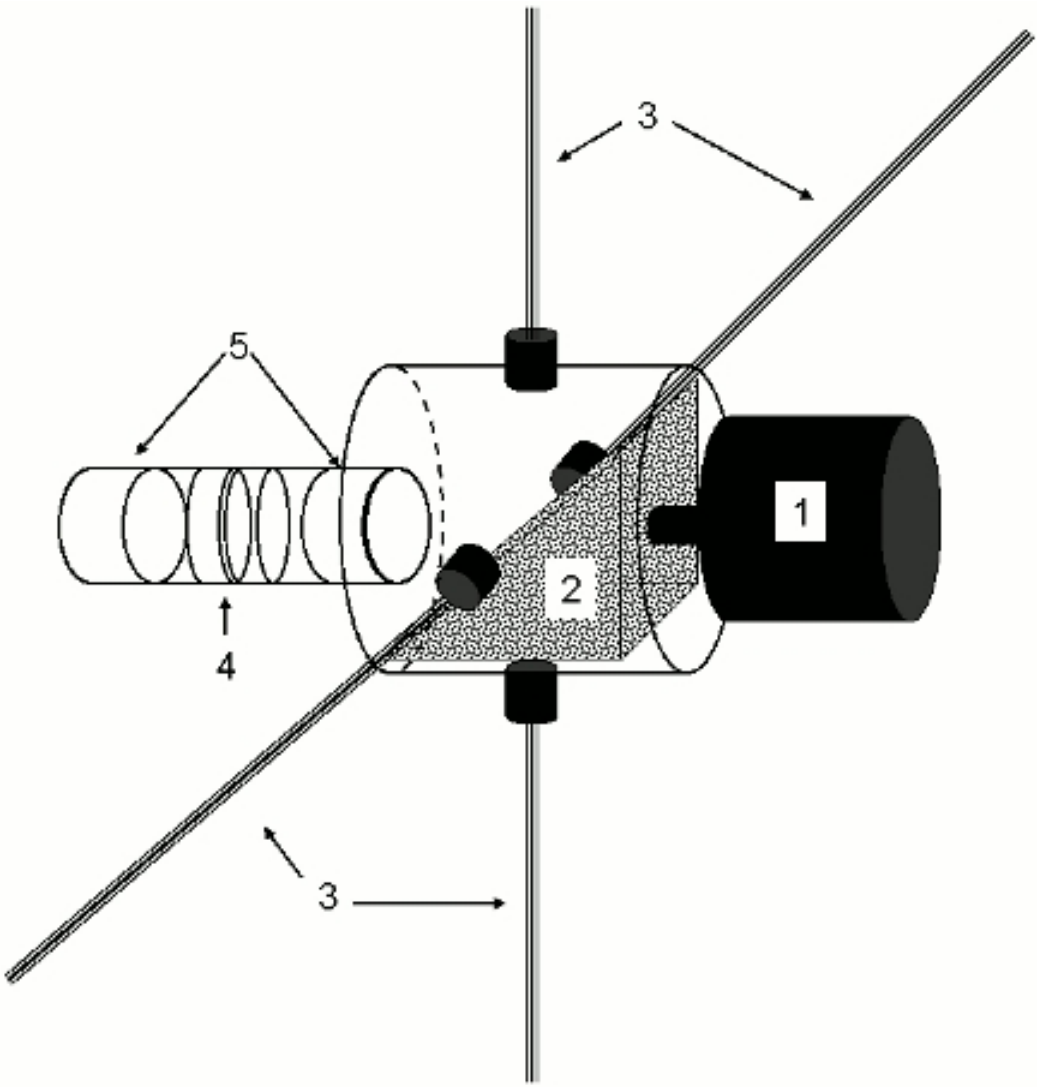

Figure 5.2: Multiplexer device which sequentially redirects the fluorescence signal from multiple sources to a single detector.

Bibliography

Acker, K., Febo, A., Trick, S., Perrino, C., Bruno, P., Wiesen, P., Moellera, D., Wieprecht, W., Auel, R., Giusto, M., Geyer, A., Platt, U., and Allegrini, I. (2006a). Nitrous acid in the urban area of rome. *Atmospheric Environment*, 40(17):3123–3133. Cited By (since 1996): 19 Export Date: 24 April 2009.

Acker, K., Moellera, D., Auel, R., Wieprecht, W., and Kalass, D. (2005). Concentrations of nitrous acid, nitric acid, nitrite and nitrate in the gas and aerosol phase at a site in the emission zone during ESCOMPTE 2001 experiment. *Atmospheric Research*, 74(1-4):507–524. Cited By (since 1996): 17 Export Date: 24 April 2009.

Acker, K., Moellera, D., Wieprecht, W., Meixner, F. X., Bohn, G., Gilge, S., Plass-Dulmer, C., and Berresheim, H. (2006b). Strong daytime production of OH from HNO_2 at a rural mountain site. *Geophysical Research Letters*, 33(2). Cited By (since 1996): 20 Export Date: 24 April 2009 Art. No.: L02809.

Akimoto, H., Takagi, H., and Sakamaki, F. (1987). Photoenhancement of

the nitrous acid formation in the surface reaction of nitrogen dioxide and water vapour: Extra radical source in smog chamber experiments. *Int. J. Chem. Kinet.*, 19:539–551. Cited By (since 1996): 22 Export Date: 22 April 2009.

Alicke, B., Geyer, A., Hofzumahaus, A., Holland, F., Konrad, S., Patz, H., Schafer, J., Stutz, J., Volz-Thomas, A., and Platt, U. (2003). OH formation by HONO photolysis during the BERLIOZ experiment. *Journal of Geophysical Research*, 108(D4).

Alicke, B., Platt, U., and Stutz, J. (2002). Impact of nitrous acid photolysis on the total hydroxyl radical budget during the LOOP/PIPAPO study in Milan. *J. Geophys. Res.*, 107(D22):8196. Cited By (since 1996): 12 Export Date: 27 April 2009 Source: Scopus.

Ammann, M., Kalberer, M., Jost, D. T., Tobler, L., Rossler, E., Piguet, D., Gaggeler, H. W., and Baltensperger, U. (1998). Heterogeneous production of nitrous acid on soot in polluted air masses. *Nature*, 395(6698):157–160. Cited By (since 1996): 131 Export Date: 27 April 2009.

Anderson, H., de Leon, A., Bland, J., Bower, J., Emberlin, J., and Strachan, D. (1998). Air pollution, pollens, and daily admissions for asthma in London 1987-92. *THORAX*, 53(10):842–848.

Atkinson, R. (2000). Atmospheric chemistry of VOCs and NOx. *Atmospheric Environment*, 34(12-14):2063–2101.

Aumont, B., Chervier, F., and Laval, S. (2003). Contribution of HONO sources to the NOx/HOx/O3 chemistry in the polluted boundary layer. *Atmospheric Environment*, 37(4):487–498. Cited By (since 1996): 51 Export Date: 17 April 2011.

Barnes, R. H. and Kircher, J. F. (1978). Laser NO_2 Fluoresence Measurements in Flames. *Applied Optics*, 17(7):1099–1102. Cited By (since 1996): 2 Export Date: 28 April 2009 Source: Scopus.

Barney, W. S. and Finlayson-Pitts, B. J. (2000). Enhancement of N_2 O_4 on Porous Glass at Room Temperature: A Key Intermediate in the Heterogeneous Hydrolysis of NO_2? *Journal of Physical Chemistry A*, 104(2):X–175. Export Date: 22 April 2009 Source: Scopus.

Bascom, R., Bromberg, P., Costa, D., Devlin, R., Dockery, D., Frampton, M., Lambert, W., Samet, J., Speizer, F., and Utell, M. (1996). Health effects of outdoor air pollution. *American Journal of Respiratory and Critical Medicine*, 153(1):3–50.

Bennett, J., Hill, A., Soleimani, A., and Edwards, W. (1975). Acute effects of combination of sulfur-dioxide and nitrogen-dioxide on plants. *Environmental Pollution*, 9(2):127–132.

Calvert, J. G., Yarwood, G., and Dunker, A. M. (1994). An evaluation of the mechanism of nitrous acid formation in the urban atmosphere. *Res. Chem.*

Intermed., 20(3-5):463–502. Cited By (since 1996): 84 Export Date: 27 April 2009.

Cleary, P. A., Wooldridge, P. J., and Cohen, R. C. (2002). Laser-induced fluorescence detection of atmospheric NO_2 with a commercial diode laser and a supersonic expansion. *Applied Optics*, 41(33):6950–6956. Cited By (since 1996): 24 Export Date: 28 April 2009 Source: Scopus.

Courtillot, I., Morville, J., Motto-Ros, V., and Romanini, D. (2006). Sub-ppb NO_2 detection by optical feedback cavity-enhanced absorption spectroscopy with a blue diode laser. *Applied Physics B-lasers and Optics*, 85(2-3):407–412.

Day, D. A., Wooldridge, P. J., Dillon, M. B., Thornton, J. A., and Cohen, R. C. (2002). A thermal dissociation laser-induced fluorescence instrument for in situ detection NO_2, peroxy nitrates, alkyl nitrates, and HNO_3. *Journal of Geophysical Research D: Atmospheres*, 107(5-6):4–1. Cited By (since 1996): 11 Export Date: 20 February 2009 Source: Scopus.

Demerjian, K. (2000). A review of national monitoring networks in North America. *Atmospheric Environment*, 34(12-14):1861–1884.

Dennekamp, M., Howarth, S., Dick, C., Cherrie, J., Donaldson, K., and Seaton, A. (2001). Ultrafine particles and nitrogen oxides generated by gas and electric cooking. *Occupational and Environmental Medicine*, 58(8):511–516.

Diamond, M. L., Gingrich, S. E., Fertuck, K., McCarry, B. E., Stern, G. A., Billeck, B., Grift, B., Brooker, D., and Yager, T. D. (2000). Evidence for organic film on an impervious urban surface: Characterization and potential teratogenic effects. *Environmental Science and Technology*, 34(14):2900–2908. Cited By (since 1996): 43 Export Date: 27 April 2009 Source: Scopus.

Donnelly, V. M. and Kaufman, F. (1978). Fluorescence lifetime studies of NO_2. II. Dependence of the perturbed 2B2 state lifetimes on excitation energy. *The Journal of Chemical Physics*, 69(4):1456–1460. Cited By (since 1996): 12 Export Date: 28 April 2009 Source: Scopus.

Fairbrother, D. H., Sullivan, D. J. D., and Johnston, H. S. (1997). Global thermodynamic atmospheric modeling: Search for new heterogeneous reactions. *Journal of Physical Chemistry A*, 101(40):7350–7358. Cited By (since 1996): 15 Export Date: 27 April 2009 Source: Scopus.

Finlayson-Pitts, B. J. (2000). *Chemistry of the upper and lower atmosphere : theory, experiments, and applications*. Academic Press, San Diego :. c2000.

Finlayson-Pitts, B. J., Wingen, L. M., Sumner, A. L., Syomin, D., and Ramazan, K. A. (2003). The heterogeneous hydrolysis of NO_2 in laboratory systems and in outdoor and indoor atmospheres: An integrated mechanism. *Physical Chemistry Chemical Physics*, 5(2):223–242. Cited By (since 1996): 94 Export Date: 22 April 2009 Source: Scopus.

Fong, C. and Brune, W. H. (1997). A laser induced fluorescence instrument for measuring tropospheric NO_2. *Review of Scientific Instruments*, 68(11):4253–4262. Cited By (since 1996): 20 Export Date: 20 February 2009 Source: Scopus.

Gao, R., Keim, E., Woodbridge, E., Ciciora, S., Proffitt, M., Thompson, T., Mclaughlin, R., and Fahey, D. (1994). New photolysis system for no2 measurements in the lower stratosphere. *Journal of Geophysical Research-Atmospheres*, 99(D10):20673–20681.

George, C., Strekowski, R. S., Kleffmann, J., Stemmler, K., and Ammann, M. (2005). Photoenhanced uptake of gaseous NO_2 on solid organic compounds: A photochemical source of HONO? *Faraday Discussions*, 130:195–210. Cited By (since 1996): 44 Export Date: 24 April 2009.

George, L. A. and O'Brien, R. J. O. (1991). Prototype FAGE determination of NO_2. *Journal of Atmospheric Chemistry*, 12(3):195–209. Cited By (since 1996): 14 Export Date: 28 April 2009 Source: Scopus.

Gillespie-Bennett, J., Pierse, N., Wickens, K., Crane, J., Howden-Chapman, P., and Res, H. H. H. S. (2011). The respiratory health effects of nitrogen dioxide in children with asthma. *European Respiratory Journal*, 38(2):303–309.

Gingrich, S. E. and Diamond, M. L. (2001). Atmospherically derived organic surface films along an urban-rural gradient. *Environmental Science and*

Technology, 35(20):4031–4037. Cited By (since 1996): 52 Export Date: 27 April 2009 Source: Scopus.

Goodman, A. L., Underwood, G. M., and Grassian, V. H. (1999). Heterogeneous Reaction of NO_2: Characterization of Gas-Phase and Adsorbed Products from the Reaction, $2NO_2$(g) + H_2O(a) -> HONO(g) + HNO_3(a) on Hydrated Silica Particles. *Journal of Physical Chemistry A*, 103(36):7217–7223. Cited By (since 1996): 56 Export Date: 27 April 2009.

Green, M. C., Xu, J., and Adhikari, N. (2008). Transport of atmospheric aerosol by gap winds in the columbia river gorge. *Journal of Applied Meteorology and Climatology*, 47(1):15–26. Cited By (since 1996): 1 Export Date: 28 April 2009 Source: Scopus.

Gutzwiller, L., Arens, F., Baltensperger, U., Gaggeler, H. W., and Ammann, M. (2002). Significance of semivolatile diesel exhaust organics for secondary hono formation. *Environmental Science and Technology*, 36(4):677–682. Cited By (since 1996): 31 Export Date: 18 May 2009 Source: Scopus.

Handley, S. R., Clifford, D., and Donaldson, D. J. (2007). Photochemical loss of nitric acid on organic films: A possible recycling mechanism for NOx. *Environmental Science and Technology*, 41(11):3898–3903.

Hard, T. M., O'Brien, R. J., Chan, C. Y., and Mehrabzadeh, A. A. (1984). Tropospheric free radical determination by FAGE. *Environmental Science*

and Technology, 18(10):768–777. Cited By (since 1996): 70 Export Date: 28 April 2009 Source: Scopus.

Harrison, R. M., Peak, J. D., and Collins, G. M. (1996). Tropospheric cycle of nitrous acid. *Journal of Geophysical Research D: Atmospheres*, 101(D9):14429–14439. Cited By (since 1996): 110 Export Date: 27 April 2009.

He, Y., Zhou, X., Hou, J., Gao, H., and Bertman, S. B. (2006). Importance of dew in controlling the air-surface exchange of HONO in rural forested environments. *Geophysical Research Letters*, 33(2). Cited By (since 1996): 5 Export Date: 24 April 2009 Art. No.: L02813.

Hodge, E. M., Diamond, M. L., McCarry, B. E., Stern, G. A., and Harper, P. A. (2003). Sticky windows: Chemical and biological characteristics of the organic film derived from particulate and gas-phase air contaminants found on an urban impervious surface. *Archives of Environmental Contamination and Toxicology*, 44(4):421–429. Cited By (since 1996): 7 Export Date: 6 May 2009 Source: Scopus.

Hoffmann, T., Odum, J., Bowman, F., Collins, D., Klockow, D., Flagan, R., and Seinfeld, J. (1997). Formation of organic aerosols from the oxidation of biogenic hydrocarbons. *Journal of Atmospheric Chemistry*, 26(2):189–222.

Hov, O. and Larssen, S. (1984). Street Canyon Concentrations of Nitrogen

Dioxide in Oslo Measurements and Model Calculations. *Environmental Science and Technology*, 18(2):82–87.

IPCC (2001). Atmospheric chemistry and greenhouse gases. *TAR*, 4:260.

Kaiser, E. W. and Wu, C. H. (1977). A kinetic study of the gas phase formation and decomposition reactions of nitrous acid. *Journal of Physical Chemistry*, 81(18):1701–1706. Cited By (since 1996): 30 Export Date: 27 April 2009.

Kebabian, P., Herndon, S., and Freedman, A. (2005). Detection of nitrogen dioxide by cavity attenuated phase shift spectroscopy. *Analytical Chemistry*, 77(2):724–728.

Kelly, T., Stedman, D., Ritter, J., and Harvey, R. (1980). Measurements of oxides of nitrogen and nitric-acid in clean-air. *Journal of Geophysical Research-Oceans and Atmospheres*, 85(NC12):7417–7425.

Kinugawa, T., Enami, S., Yabushita, A., Kawasaki, M., Hoffmann, M. R., and Colussi, A. J. (2011). Conversion of gaseous nitrogen dioxide to nitrate and nitrite on aqueous surfactants. *Physical Chemistry Chemical Physics*, 13(11):5144–5149.

Kleffmann, J., Benter, T., and Wiesen, P. (2004). Heterogeneous reaction of nitric acid with nitric oxide on glass surfaces under simulated atmospheric conditions. *Journal of Physical Chemistry A*, 108(27):5793–5799.

Kleffmann, J., Gavriloaiei, T., Hofzumahaus, A., Holland, F., Koppmann, R., Rupp, L., Schlosser, E., Siese, M., and Wahner, A. (2005). Daytime formation of nitrous acid: A major source of OH radicals in a forest. *Geophysical Research Letters*, 32(5):1–4. Cited By (since 1996): 36 Export Date: 24 April 2009.

Kley, D. and McFarland, M. (1980). Chemiluminescence detector for no and no2. *Journal Name: Atmos. Technol.; (United States); Journal Volume: 12*, pages Medium: X; Size: Pages: 63–69.

Knipping, E. M. and Dabdub, D. (2002). Modeling surface-mediated renoxification of the atmosphere via reaction of gaseous nitric oxide with deposited nitric acid. *Atmospheric Environment*, 36(36-37):5741–5748. Cited By (since 1996): 11 Export Date: 27 April 2009 Source: Scopus.

Kotamarthi, V. R., Gaffney, J. S., Marley, N. A., and Doskey, P. V. (2001). Heterogeneous nox chemistry in the polluted pbl. *Atmospheric Environment*, 35(26):4489–4498. Cited By (since 1996): 13 Export Date: 27 April 2009 Source: Scopus.

Lammel, G. and Cape, J. N. (1996). Nitrous acid and nitrite in the atmosphere. *Chemical Society Reviews*, 25(5):361–369. Cited By (since 1996): 109 Export Date: 27 April 2009.

Li, Y., Demerjian, K., Zahniser, M., Nelson, D., McManus, J., and Herndon, S. (2004). Measurement of formaldehyde, nitrogen dioxide, and sulfur

dioxide at Whiteface Mountain using a dual tunable diode laser system. *Journal of Geophysical Research-Atmospheres*, 109(D16).

Linn, W., Szlachcic, Y., Gong, H., Kinney, P., and Berhane, K. (2000). Air pollution and daily hospital admissions in metropolitan Los Angeles. *Environmental Health Perspectives*, 108(5):427–434.

Liu, Q. T., Chen, R., McCarry, B. E., Diamond, M. L., and Bahavar, B. (2003). Characterization of polar organic compounds in the organic film on indoor and outdoor glass windows. *Environmental Science and Technology*, 37(11):2340–2349. Cited By (since 1996): 16 Export Date: 6 May 2009 Source: Scopus.

Logan, J. A. (1983). Nitrogen oxides in the troposphere: global and regional budgets. *Journal of Geophysical Research*, 88(C15):10785–10807. Cited By (since 1996): 200 Export Date: 27 April 2009 Source: Scopus.

Macmanus, J., Kebabian, P., and Zahniser, W. (1995). Astigmatic mirror multipass absorption cells for long-path-length spectroscopy. *Applied Optics*, 34(18):3336–3348.

Mann, B. A., White, R. F., and Morrison, R. J. S. (1996). Detection and imaging of nitrogen dioxide with the degenerate four-wave-mixing and laser-induced-fluorescence techniques. *Applied Optics*, 35(3):475–481. Cited By (since 1996): 13 Export Date: 20 February 2009 Source: Scopus.

Matsumi, Y., Murakami, S. I., Kono, M., and Takahashi, K. (2001). High-sensitivity instrument for measuring atmospheric NO_2. *Analytical Chemistry*, 73(22):5485–5493. Cited By (since 1996): 17 Export Date: 20 February 2009 Source: Scopus.

McKinnon, I. R., Mathieson, J. G., and Wilson, I. R. (1979). Gas phase reaction of nitric oxide with nitric acid. *The Journal of Physical Chemistry*, 83(7):779–780. Cited By (since 1996): 5 Export Date: 17 April 2011.

Mochida, M. and Finlayson-Pitts, B. J. (2000). FTIR studies of the reaction of gaseous NO with HNO_3 on porous glass: Implications for conversion of HNO_3 to photochemically active NO_x in the atmosphere. *Journal of Physical Chemistry A*, 104(43):9705–9711. Cited By (since 1996): 30 Export Date: 22 April 2009 Source: Scopus.

Mouri, H., Okada, K., and Takahashi, S. (1995). Giant sulfur dominant particles in remote marine boundary layer. *Geophysical Research Letters*, 22(5):595–598.

Moussiopoulos, N., Papalexiou, S., Lammel, G., and Arvanitis, T. (2000). Simulation of nitrous acid formation taking into account heterogeneous pathways: Application to the milan metropolitan area. *Environmental Modelling and Software*, 15(6-7 SPEC. ISS):629–637. Cited By (since 1996): 7 Export Date: 18 May 2009 Source: Scopus.

Moxim, W. (1990). Simulated transport of noy to hawaii during

august- a synoptic study. *Journal of Geophysical Research-Atmospheres*, 95(D5):5717–5729.

Orlando, J., Tyndall, G., Moortgat, G. K., and Calvert, J. G. (1993). Quantum Yields for NO_3 Photolysis Between 570 and 635 nm. *Journal of Physical Chemistry*, 97(42):10996–11000.

Osthoff, H. D., Brown, S. S., Ryerson, T. B., Fortin, T. J., Lerner, B. M., Williams, E. J., Pettersson, A., Baynard, T., Dube, W. P., Ciciora, S. J., and Ravishankara, A. R. (2006). Measurement of atmospheric NO_2 by pulsed cavity ring-down spectroscopy. *Journal of Geophysical Research-Atmospheres*, 111(D12).

Parra, J. and George, L. A. (2009). Development of an ambient pressure laser-induced fluorescence instrument for nitrogen dioxide. *Applied Optics*, 48(18):3355–3361. Export Date: 3 May 2010 Source: Scopus.

Perner, D. and Platt, U. (1979). Detection of nitrous acid in the atmosphere by differential optical absorption. *Geophysical Research Letters*, 6(12):917–920. Cited By (since 1996): 95 Export Date: 27 April 2009.

Platt, U. and Perner, D. (1980). Direct measurements of atmospheric CH_2O,HNO_2,O_3,NO_2, and SO_2 by differential optical-absorption in the near UV. *Journal of Geophysical Research-Oceans and Atmospheres*, 85(NC12):7453–7458.

Pollack, I. B., Lerner, B. M., and Ryerson, T. B. (2010). Evaluation of ultraviolet light-emitting diodes for detection of atmospheric NO_2 by photolysis - chemiluminescence. *Journal of Atmospheric Chemistry*, 65(2-3):111–125.

Ramazan, K. A., Syomin, D., and Finlayson-Pitts, B. J. (2004). The photochemical production of HONO during the heterogeneous hydrolysis of NO_2. *Physical Chemistry Chemical Physics*, 6(14):3836–3843. Cited By (since 1996): 31 Export Date: 22 April 2009 Source: Scopus.

Ramazan, K. A., Wingen, L. M., Miller, Y., Chaban, G. M., Gerber, R. B., Xantheas, S. S., and Finlayson-Pitts, B. J. (2006). New experimental and theoretical approach to the heterogeneous hydrolysis of NO_2: Key role of molecular nitric acid and its complexes. *Journal of Physical Chemistry A*, 110(21):6886–6897. Cited By (since 1996): 22 Export Date: 22 April 2009 Source: Scopus.

Reich, P., Ellsworth, D., Kloeppel, B., Fownes, J., and Gower, S. (1990). Vertical Variation in Canopy Structure and CO_2 exchange of Oak-Maple Forests- Influence of Ozone, Nitrogen, and Other Factors on Simulated Canopy Carbon Gain. *Tree Physiology*, 7(1-4):329–345. WORKSHOP ON DYNAMICS OF ECOPHYSIOLOGICAL PROCESSES IN TREE CROWNS AND FOREST CANOPIES, RHINELANDER, WI, SEP, 1989.

Ridley, B., Carroll, M., Gregory, G., and Sachse, G. (1988). NO and nNO2 in the troposphere - technique and measurements in regions of

a folded tropopause. *Journal of Geophysical Research-Atmospheres*, 93(D12):15813–15830.

Rivera-Figueroa, A. M., Sumner, A. L., and Finlayson-Pitts, B. J. (2003). Laboratory studies of potential mechanisms of renoxification of tropospheric nitric acid. *Environmental Science and Technology*, 37(3):548–554. Cited By (since 1996): 25 Export Date: 27 April 2009 Source: Scopus.

Saliba, N. A., Mochida, M., and Finlayson-Pitts, B. J. (2000). Laboratory studies of sources of HONO in polluted urban atmospheres. *Geophysical Research Letters*, 27(19):3229–3232. Cited By (since 1996): 34 Export Date: 22 April 2009 Source: Scopus.

Saliba, N. A., Yang, H., and Finlayson-Pitts, B. J. (2001). Reaction of gaseous nitric oxide with nitric acid on silica surfaces in the presence of water at room temperature. *Journal of Physical Chemistry A*, 105(45):10339–10346. Cited By (since 1996): 35 Export Date: 27 April 2009 Source: Scopus.

Salisbury, G., Rickard, A., Monks, P., Allan, B., Bauguitte, S., Penkett, S., Carslaw, N., Lewis, A., Creasey, D., Heard, D., Jacobs, P., and Lee, J. (2001). Production of peroxy radicals at night via reactions of ozone and the nitrate radical in the marine boundary layer. *Journal of Geophysical Research-Atmospheres*, 106(D12):12669–12687.

Schierhorn, K., Zhang, M., Matthias, C., and Kunkel, G. (1999). Influence

of ozone and nitrogen dioxide on histamine and interleukin formation in a human nasal mucosa culture system. *AMERICAN JOURNAL OF RESPIRATORY CELL AND MOLECULAR BIOLOGY*, 20(5):1013–1019.

Schiller, C. L., Locquiao, S., Johnson, T. J., and Harris, G. W. (2001). Atmospheric measurements of hono by tunable diode laser absorption spectroscopy. *Journal of Atmospheric Chemistry*, 40(3):275–293. Cited By (since 1996): 17 Export Date: 27 April 2009.

Schneider, W., Moortgat, G. K., Tyndall, G., and Burrows, J. (1987). Absorption cross-sections of NO_2 in the UV and visible region (200 - 700 nm) at 298-K. *Journal of Photochemistry and Photobiology A: Chemistry*, 40(2-3):195–217.

Singh, H. B., Viezee, W., Chen, Y., Thakur, A. N., Kondo, Y., Talbot, R. W., Gregory, G. L., Sachse, G. W., Blake, D. R., Bradshaw, J. D., Wang, Y., and Jacob, D. J. (1998). Latitudinal distribution of reactive nitrogen in the free troposphere over the pacific ocean in late winter/early spring. *Journal of Geophysical Research D: Atmospheres*, 103(D21):28237–28246. Cited By (since 1996): 30 Export Date: 27 April 2009 Source: Scopus.

Sivakumaran, V., Subramanian, K. P., and Kumar, V. (2001a). Lifetime measurements of NO_2 in the predissociation region 399-416 nm. *Journal of Quantitative Spectroscopy and Radiative Transfer*, 69(4):519–524. Cited By (since 1996): 2 Export Date: 28 April 2009 Source: Scopus.

Sivakumaran, V., Subramanian, K. P., and Kumar, V. (2001b). Self-quenching and zero-pressure lifetime studies of NO_2 at 465-490, 423-462 and 399-416 nm. *Journal of Quantitative Spectroscopy and Radiative Transfer*, 69(4):525–534. Cited By (since 1996): 6 Export Date: 28 April 2009 Source: Scopus.

Smith, A., Hall, G., Whitaker, B., Astill, A., Neyer, D., and Delve, P. (1995). Effects of Inert-Gases on the Degenerate 4-Wave-Mixing Spectrum of NO_2. *Applied Physics B-Lasers and Optics*, 60(1):11–18.

Smith, J. H. (1947). A rate study of the oxidation of nitric oxide with nitric acid vapor. *Journal of the American Chemical Society*, 69(7):1741–1747. Cited By (since 1996): 10 Export Date: 17 April 2011.

Soergel, M., Regelin, E., Bozem, H., Diesch, J. M., Drewnick, F., Fischer, H., Harder, H., Held, A., Hosaynali-Beygi, Z., Martinez, M., and Zetzsch, C. (2011). Quantification of the unknown HONO daytime source and its relation to NO_2. *Atmospheric Chemistry and Physics*, 11(20):10433–10447.

Streit, G. E., Wells, J. S., Fehsenfeld, F. C., and Howard, C. J. (1979). A tunable diode laser study of the reactions of nitric and nitrous acids: HNO_3+NO and HNO_2+O3. *The Journal of Chemical Physics*, 70(7):3439–3443. Cited By (since 1996): 9 Export Date: 17 April 2011.

Stutz, J., Alicke, B., and Neftel, A. (2002). Nitrous acid formation in the urban atmosphere: Gradient measurements of NO and HONO over grass

in Milan, Italy2. *J. Geophys. Res.*, 107(D22):8192–8207. Cited By (since 1996): 8 Export Date: 27 April 2009 Source: Scopus.

Svensson, R., Ljungstrom, E., and Lindqvist, O. (1987). Kinetics of the reaction between nitrogen dioxide and water vapour. *Atmospheric Environment*, 21(7):1529–1539. Cited By (since 1996): 78 Export Date: 17 April 2011.

Taketani, F., Kawai, M., Takahashi, K., and Matsumi, Y. (2007). Trace detection of atmospheric no2 by laser-induced fluorescence using a gan diode laser and a diode-pumped yag laser. *Applied Optics*, 46(6):907–915. Cited By (since 1996): 4 Export Date: 28 April 2009 Source: Scopus.

Teklemariam, T. A. and Sparks, J. P. (2006). Leaf fluxes of NO and NO_2 in four herbaceous plant species: The role of ascorbic acid. *Atmospheric Environment*, 40(12):2235–2244. Cited By (since 1996): 4 Export Date: 18 May 2009 Source: Scopus.

Thornton, J. A., Wooldridge, P. J., and Cohen, R. C. (2000). Atmospheric NO_2: In Situ laser-induced fluorescence detection at parts per trillion mixing ratios. *Analytical Chemistry*, 72(3):528–539. Cited By (since 1996): 73 Export Date: 28 April 2009 Source: Scopus.

Tunnicliffe, W., Burge, P., and Ayres, J. (1994). Effect of domestic concentrations of nitrogen-dioxide on airway responses to inhaled allergen in asthmatic-patients. *Lancet*, 344(8939-4):1733–1736.

Weinberger, B., Laskin, D., Heck, D., and Laskin, J. (2001). The toxicology of inhaled nitric oxide. *Toxicological Sciences*, 59(1):5–16.

Williams, E. J., Baumann, K., Roberts, J. M., Bertman, S. B., Norton, R. B., Fehsenfeld, F. C., Springston, S. R., Nunnermacker, L. J., Newman, L., Olszyna, K., Meagher, J., Hartsell, B., Edgerton, E., Pearson, J. R., and Rodgers, M. O. (1998). Intercomparison of ground-based noy measurement techniques. *Journal of Geophysical Research D: Atmospheres*, 103(D17):22261–22280. Cited By (since 1996): 51 Export Date: 28 April 2009 Source: Scopus.

Winer, A., Peters, J., Smith, J., and Pitts, J. (1974). Response of commercial chemiluminescent NO-NO_2 analyzers to other nitrogen-containing compounds. *Environmental Science & Technology*, 8(13):1118–1121.

Winer, A. M. and Biermann, H. W. (1994). Long pathlength differential optical absorption spectroscopy (D O A S) measurements of gaseous HONO, NO_2 and HCNO in the California South Coast Air Basin. *Research on Chemical Intermediates*, 20(3-5):423–445. Cited By (since 1996): 56 Export Date: 17 April 2011.

Zhou, X., Zhang, N., TerAvest, M., Tang, D., Hou, J., Bertman, S., Alaghmand, M., Shepson, P. B., Carroll, M. A., Griffith, S., Dusanter, S., and Stevens, P. S. (2011). Nitric acid photolysis on forest canopy surface as a source for tropospheric nitrous acid. *Nature Geoscience*, 4(7):440–443.

Ziemba, L. D., Dibb, J. E., Griffin, R. J., Anderson, C. H., Whitlow, S. I., Lefer, B. L., Rappenglueck, B., and Flynn, J. (2010). Heterogeneous conversion of nitric acid to nitrous acid on the surface of primary organic aerosol in an urban atmosphere. *ATMOSPHERIC ENVIRONMENTAtmospheric Environment*, 44(33, SI):4081–4089.